High-Power Electronic Applications Enabled by Medium Voltage Silicon-Carbide Technology: An Overview

Morten Rahr Nielsen, *Graduate Student Member, IEEE*, Shiyue Deng, *Graduate Student Member, IEEE*, Abdul Basit Mirza, *Graduate Student Member, IEEE*, Benjamin Futtrup Kjærsgaard, *Graduate Student Member, IEEE*, Asger Bjørn Jørgensen, Hongbo Zhao, *Member, IEEE*, Yang Li, *Graduate Student Member, IEEE*, Stig Munk-Nielsen, *Member, IEEE*, and Fang Luo, *Senior Member, IEEE*

***Abstract*—With the electrification of society and the green transition, the need for efficient high-power electronic converters to support the electricity demand is at an all-time high. A key enabler is the emerging medium voltage (MV) silicon-carbide (SiC) semiconductor devices, which offer improved static and dynamic performance compared to their silicon-counterparts. This article presents a thorough overview of the recent advancements within the MV SiC technology, examining both available semiconductor devices and power modules from industry and academia and directly associates them to their applicability through a comprehensive review of typical high-power electronic applications. At last, the future perspectives on the applicability and commercial widespread of the MV SiC technology are presented.**

***Index Terms*—Commercialization of medium-voltage (MV) silicon carbide (SiC), insulated-gate bipolar transistor (IGBT), MOSFET, overview of applicability, perspectives, policy-making.**

I. Introduction

ELECTRIFICATION of society elevates the global demand for renewable energy as processes previously relying on fossil fuels are being replaced by more sustainable alternatives [1]. Heat pumps and electric vehicles (EVs) are some of the applications hereof that have experienced a large increase in interest within the previous years [2], [3], [4], [5]. In parallel with the electrification of society, the green transition has further elevated the production of renewable energy from wind and solar [2], [3], [4], [5], [6] but also elevated the consumption of renewable energy for the production of green hydrogen through electrolysis [2], [3], [4], [5] and for large data centers [2]. In this context, efficient power electronic converters (PEC) for high-power applications, above hundreds of kilowatts, are essential to support the increasing societal demand for energy, as they provide efficient control and conversion of energy.

A thorough study of released and announced industrial PEC products for high-power electronic applications has been conducted within the above-mentioned applications since 2010 and categorized as follows: EV charging of light (e.g., scooters and cars) and heavy transport (e.g., buses, trucks, and vessels), uninterruptible power supplies, and power distribution units for data centers, power supplies for electrolyzer units, medium voltage (MV) motor drives, central inverters used in photovoltaics (PVs), and converters from wind turbines, as shown in Fig. 1. Rough trendlines for each application have been added to the figure.

Each of the applications shows a clear positive trend of an increasing interest in releasing products with higher power ratings. Although most of the presented high-power PECs are based on low-voltage (LV) technology, several high-power PECs based on MV technology have been released within applications of wind turbines and motor drives.

The term "MV" has multiple definitions depending on the context. The international standard IEC60038 [91] defines the MVAC range from 1 to 35 kV, whereas national standards (e.g., ANSI [92]) have different definitions (i.e., 0.6–69 kV). The authors follow the established consensus of defining MV semiconductor devices and power modules starting from 3.3 kV in blocking voltage [93], [94], [95].

Historically, MV semiconductor devices for high-power electronic applications have been dominated by thyristors, and diodes, since the 1960s [96], [97], [98] where they replaced the conventional mercury-arc rectifiers [99]. During the 1970s,

Received 8 May 2024; revised 29 June 2024; accepted 5 August 2024. Date of publication 13 August 2024; date of current version 12 December 2024. This work was supported in part by the MVolt and in part by the ComElCo. MVolt was supported in part by the AAU Energy at Aalborg University, in part by the Innovation Fund Denmark, in part by the Siemens Gamesa Renewable Energy, in part by the Vestas Wind Systems, in part by the KK Wind Solutions. ComElCo was supported by the Innovation Fund Denmark under Grant 1150-00001B under Mission Green Fuels, and in part by the U.S. National Science Foundation under Grant 2143112. Recommended for publication by Associate Editor M. Narimani. *(Corresponding author: Fang Luo.)*

Morten Rahr Nielsen, Asger Bjørn Jørgensen, Hongbo Zhao, and Stig Munk-Nielsen are with the AAU Energy, Aalborg University, 9220 Aalborg, Denmark (e-mail: mrni@energy.aau.dk; abj@energy.aau.dk; hzh@energy.aau.dk; smn@energy.aau.dk).

Shiyue Deng, Yang Li, and Fang Luo are with the Department of Electrical and Computer Engineering, Stony Brook University, Stony Brook, NY 11794-0701 USA (e-mail: shiyue.deng@stonybrook.edu; yang.li.9@stonybrook.edu; fang.luo@stonybrook.edu).

Abdul Basit Mirza was with the Department of Electrical and Computer Engineering, Stony Brook University, Stony Brook, NY 11794-0701 USA. He is now with the Eaton Research Lab, Menomonee Falls, WI 53051-4404 USA (e-mail: abdulbasit.mirza@ieee.org).

Benjamin Futtrup Kjærsgaard was with the AAU Energy, Aalborg University, 9220 Aalborg, Denmark. He is now with the PowerCon A/S, 9500 Hobro, Denmark (e-mail: benjamin.futtrup.kjaersgaard@powercon.dk).

Color versions of one or more figures in this article are available at https://doi.org/10.1109/TPEL.2024.3442483.

Digital Object Identifier 10.1109/TPEL.2024.3442483

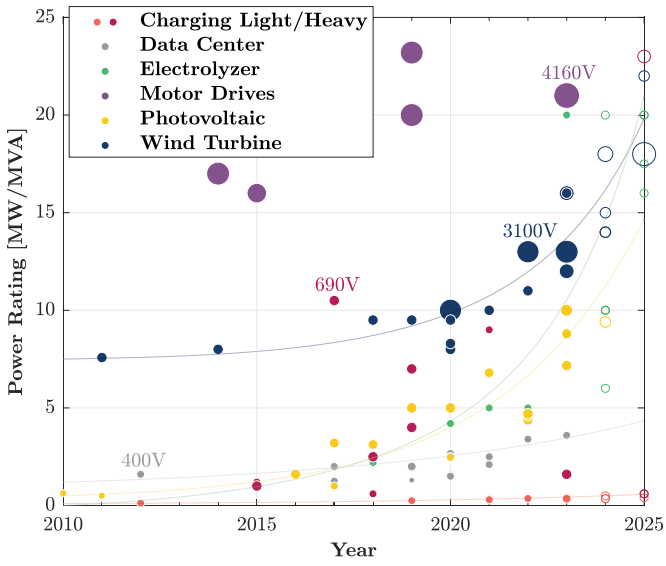

Fig. 1. Overview of released and announced industrial power electronics converters for high-power applications. Size indicates the AC voltage of the converter side, filled indicates a released product, and hollow indicates an announced product. Data source: EV charging (light [7], [8], [9], [10], [11], [12], [13], [14], [15], [16], [17] and heavy [18], [19], [20], [21], [22], [23], [24], [25], [26], [27], [28], [29]), data center [30], [31], [32], [33], [34], [35], [36], [37], [38], [39], [40], [41], [42], [43], electrolyzers [44], [45], [46], [47], [48], [49], [50], [51], [52], [53], [54], [55], [56], [57], motor drives [58], [59], [60], PVs [61], [62], [63], [64], [65], [66], [67], [68], [69], [70], [71], [72], [73], [74], [75], and wind turbines [76], [77], [78], [79], [80], [81], [82], [83], [84], [85], [86], [87], [88], [89], [90].

a breakthrough happened with the introduction of the gate turn-OFF (GTO) thyristors, which featured a "self-turn-OFF" feature [99]. Although multiple variants of thyristors existed in the late 1990s [96], the integrated gate-commutated thyristor (IGCT), an advanced GTO [98], was deemed the optimum thyristor technology for MV high-power electronic applications [97], [98] due to their superior static performance and reliability. Even though the silicon (Si) insulated-gate bipolar transistor (IGBT) was already invented in the early 1980s, the first MV power module based on MV Si IGBTs intended for high-power electronic applications (4.5 kV–2000 A) was first presented in 2000 by Fuji Electric Co. [100] with the potential of challenging the IGCTs in MV high-power electronic applications [101]. Since then, IGCTs and Si IGBTs have coexisted and become state-of-the-art for MV semiconductor devices [99].

With the recent advancements in the emerging wide bandgap (WBG) semiconductor materials, an attractive alternative to the state-of-the-art Si technology is the silicon-carbide (SiC) technology, which exploits the opportunity of not only manufacturing IGBTs and GTOs but also MOSFETs with increased breakdown voltages at and above 3.3 kV. Intrinsic to the material properties of SiC, the SiC semiconductor devices present higher breakdown voltage capabilities, improved switching performance, and stable performance at high temperatures compared to their Si-counterparts [102], [103].

An alternative to MV semiconductor devices is multilevel typologies and series connected configurations of LV semiconductor devices. Multilevel typologies have matured for more than 40 years since the invention of the first three-level typology [104]. Since then, several advanced multilevel typologies, including the modular multilevel converter (MMC), have been proposed in the literature and put into practical use for various medium to high voltage applications [105], [106], [107]. However, multilevel typologies will not be discussed in detail as the prime focus is the availability and adoption of MV SiC semiconductor devices and power modules.

Several research overview papers [93], [95], [108], [109] from 2022 or earlier discuss the development and applicability of MV SiC semiconductor devices in various levels of detail. A comprehensive comparative and up-to-date overview of the recent advancements within the emerging MV SiC technology is, therefore, missing in the literature. The MV SiC technology has experienced significant advancements in recent years, not only with the introduction of the first commercially available MV SiC semiconductor devices from Wolfspeed, GeneSiC, and Microchip, but also from the increasing interest from industry and academia to design high-performance power modules, which paves the way for full utilization and exploration of the emerging technology.

The rest of this article is organized as follows. An overview of the MV SiC technology and its recent advancements are presented in Section II together with exhaustive lists of available MV SiC semiconductor dies and power modules from both industry and academia. This is followed in Section III by a thorough review of typical high-power electronic applications enabled by recent advancements in the MV SiC technology and highlight the unique benefits. Sections IV is addressing future perspectives related to the applicability and commercial widespread of the MV SiC technology from our perspective. Finally, Section V concludes this article.

II. MV SiC Technology

The SiC technology, and WBG technologies in general, present superior materials properties compared to its Si-counterpart and has, therefore, been heavily studied in the last decade [102], [103], [110], [111]. The literature already presents highly detailed information regarding the SiC material properties, crosssectional device structures, and the different device types and thoroughly benchmarks them theoretically to the state-of-the-art Si semiconductor devices in terms of their static and dynamic performance [102], [103], [110], [111]. Currently, the well-established Si technology is limited in its breakdown voltage capability, operations temperature, and switching frequency by its material properties, and as a direct consequence of this, power modules with Si IGBTs are topped at a breakdown voltage of 6.5 kV with a limited switching performance [102]. Although the SiC technology theoretically presents improved static and dynamic performance compared to the Si technology, the SiC technology for MV applications is still in an early maturity stage, and as a result, the majority of the MV SiC semiconductor devices are currently only manufactured as engineering samples. The most common engineering samples of MV SiC semiconductor devices are MOSFETs, IGBTs, and GTOs; however, junction gate field-effect transistors (JFETs), bipolar

TABLE I
OVERVIEW OF MV SiC SEMICONDUCTOR DEVICES WITH AVAILABLE DATA OF JUN. 2024

Year	Affiliation	Device	Breakdown voltage (kV)	Forward current (A)	ON-resistance (mΩ)	Forward voltage (V)	Die size (cm^2)	Active area (cm^2)	Turn-ON energy (mJ)	Turn-OFF energy (mJ)	Ref.
2014	Cree‡	MOSFET	3.3	25	38	–	0.47	0.28	0.7	0.6	[118]
2015	Mitsubishi‡	MOSFET	3.3	30	57†	–	0.36	–	–	–	[125]
2016	Wolfspeed‡	MOSFET	3.3	48	40	–	0.43	–	35*	8*	[128], [129]
2017	ROHM‡	MOSFET	3.3	50	30	–	0.52	0.41	55*	36*	[126]
2019	GeneSiC‡	MOSFET	3.3	50	40	–	0.43	–	15.5	2	[130]
2021	GeneSiC	MOSFET	3.3	49	50	–	0.43†	–	3.3†	3.8†	G2R50MT33-CAL
2022	Microchip	MOSFET	3.3	66	25	–	0.67	0.37†	–	–	MSC025SMA330D/S
2023	Wolfspeed	MOSFET	3.3	52	53	–	0.38	0.25	–	–	CPM3-3300-R050
2014	USCi‡	JFET	6.5	15	340	–	0.36	–	7.2	2.3	[131]
2015	Wolfspeed‡	MOSFET	6.5	30	100	–	0.71	–	5.5	0.6	[132]
2017	Wolfspeed‡	MOSFET	6.5	30	88	–	0.66	0.41	12.1	1.7	[132]
2017	ROHM‡	MOSFET	6.5	30	129	–	0.52	0.35	75*	26*	[126]
2020	GeneSiC‡	MOSFET	6.5	10	325	–	–	–	–	–	G2R325MS65-CAL
2020	GeneSiC‡	MOSFET	6.5	10	300	–	–	–	–	–	G2R300MT65-CAL
2021	Hitachi‡	MOSFET	6.5	12	–	–	–	–	16	5	[127], [133]
2006	Cree‡	MOSFET	10	5	670	–	0.30	0.15	–	–	[134], [135]
2008	Cree‡	MOSFET	10	10	410	–	0.66	0.31	4.5	0.8	[116], [121]
2010	Cree‡	BJT	10	10	390	–	0.75	0.34	–	–	[136]
2013	GeneSiC‡	BJT	10	8	–	–	0.53	0.28	4.2	1.6	[137]
2014	Cree‡	MOSFET	10	20	350	–	0.66	0.39	8.4	1.3	[117], [120]
2018	Wolfspeed‡	MOSFET	10	20	300	–	0.66†	–	–	–	[138]
2021	Hitachi‡	MOSFET	10	10	–	–	–	–	27	12	[127], [133]
2009	Cree‡	IGBT	13	–	49†	3	0.45†	–	–	–	[139]
2012	Cree‡	IGBT	12.5	5	33	4.1	0.45	0.16	–	15†	[140], [141]
2012	Cree‡	GTO	12	50	6.9†	3.97	1.00	0.58	–	–	[142]
2013	Japan AIST‡	IGBT	16	2†	125	5	0.09	0.02†	–	–	[143]
2013	Cree‡	IGBT	15	20	100†	6	0.71	0.32	–	–	[122], [141]
2014	Cree‡	MOSFET	15	10	650	–	0.64	0.32	8.9	1.9	[118]
2014	Wolfspeed‡	MOSFET	15	10	300	–	0.64	0.32	10.2	3	[120]
2014	Japan AIST‡	IGBT	16	11	125†	5.1	0.28	0.11	–	–	[123], [144]
2018	Nanjing NEDI‡	IGBT	13	25†	130†	9†	–	1.06	–	–	[145]
2019	Cree‡	GTO	15	46.5†	–	5.18	1.00	0.47	–	–	[146]
2010	Purdue U.‡	IGBT	20	–	–	3	–	–	–	–	[147]
2013	Cree‡	IGBT	20.7	20	66†	6.4	1.00	0.42	–	–	[148]
2014	Cree‡	IGBT	22	20	22	7.5	1.00	0.37	–	34	[149], [150]
2014	Cree‡	GTO	20	53†	14.5†	4†	2.00	0.53	–	–	[119], [151]
2014	Cree‡	IGBT	27	20	–	11.8	0.81	0.28	–	28†	[119], [152]

‡Engineering sample †Estimated value *Specified at T_j of 125°C
All values are specified at room temperature unless otherwise specified.

junction transistors (BJTs), and supercascode (SC) structures do also exist [93], [94], [95], [109], [111], [112], [113].

Further advancements of the MV SiC technology include but are not limited to improved manufacturing techniques such as trench gate and CoolMOS structures for MOSFETs [93] and improved packaging technologies to adhere to the insulation requirement and to limit the impact of parasitics [94]. According to Baliga [114], future developments also focus on a further increase in the breakdown voltage to expand the application area to even higher voltage levels.

A comprehensive overview of available MV SiC semiconductor devices and power modules is given in the subsequent sections and serves as a guideline for choosing the most suitable semiconductor device or power module for MV applications.

A. SiC Semiconductor Devices

There exist only a limited amount of commercially available MV SiC semiconductor devices; however, multiple well-renowned companies and research institutes can manufacture MV SiC semiconductor devices as engineering samples. An exhaustive list of single-die MV SiC semiconductor devices, both commercially available and engineering samples, are presented in Table I and ordered in terms of their breakdown voltage and announced year. No inquiry-protected information is included in the table. The list has been limited to normally OFF semiconductor devices intended for high-power electronic applications, which exclude all types of *p*-channel devices and semiconductor devices with a rated forward current of less than 1 A. In addition, the list has been narrowed down to SiC IGBTs and GTOs with breakdown voltages above 10 kV. Multiple companies and research institutes have additional MV SiC semiconductor devices in the pipeline, but not officially announced, and therefore, not included in the table.

A cross-comparison between all types of MV SiC semiconductor devices has been performed in terms of their static and dynamic performance as well as their size properties.

1) From the comparison of their static performance (current density versus breakdown voltage) shown in Fig. 2, it is evident that SiC IGBTs and GTOs present an improved

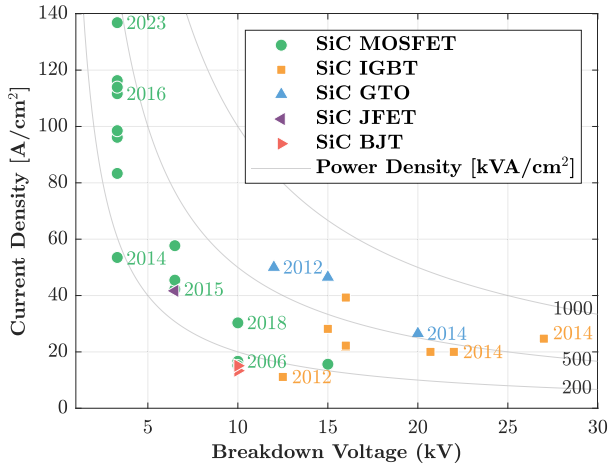

Fig. 2. Static performance of MV SiC semiconductor devices.

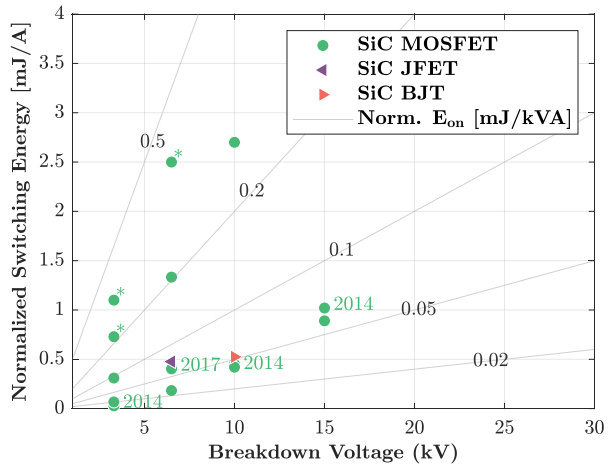

Fig. 3. Turn-ON performance of MV SiC semiconductor devices. *Specified at T_j of 125 °C.

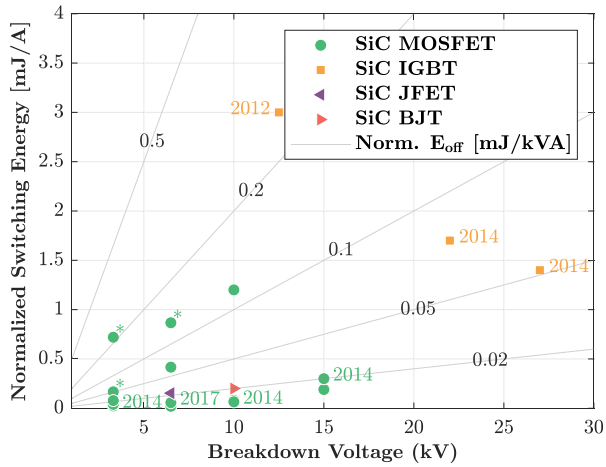

Fig. 4. Turn-OFF performance of MV SiC semiconductor devices. *Specified at T_j of 125 °C.

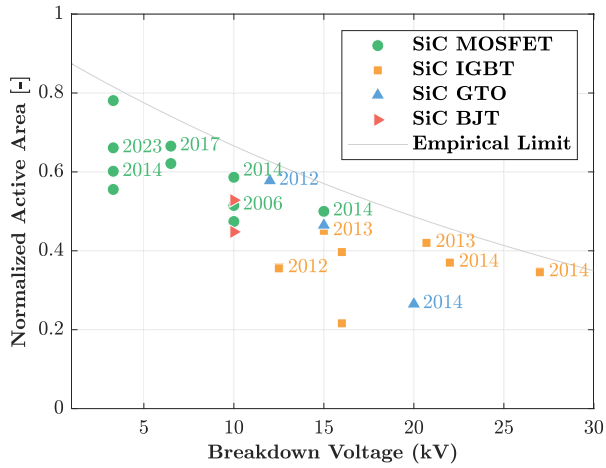

Fig. 5. Normalized active area of MV SiC semiconductor devices.

power density compared to SiC MOSFETs throughout the whole voltage range in accordance with the simulation study of the theoretical performance for MV SiC MOSFETs, IGBTs, and GTOs [115]. The findings are supported by the existing literature in which several studies cross-compare the maximum power capability among MV Si IGBTs, SiC IGBTs, and SiC MOSFETs [116], [117], [118], [119], [120].

2) The comparison further includes their dynamic performance (normalized turn-ON/OFFenergy versus breakdown voltage) shown in Figs. 3 and 4 for those MV SiC semiconductor devices that have readily available switching energies or waveforms. To make a fair comparison throughout the whole voltage range, the included switching energies are collected at 50%–60% of rated breakdown voltage [103] and at approx. its rated forward current. However, the comparison does not consider differences in dv/dt, di/dt, gate resistances, or test setups, which inevitably impacts the accuracy of the comparison. In the existing literature, several studies cross-compare the switching performance among MV Si IGBTs, SiC IGBTs, and SiC MOSFETs [118], [119], [120], [121], [122], [123], [124], [125], [126], [127] under certain test conditions. In general, SiC MOSFETs and SiC IGBTs present a 70%–90% [125], [126], [127] and 35%–60% [123] reduction in switching energies, respectively, compared to Si IGBTs under similar test conditions.

3) At last, the comparison presents the active area normalized to its die size (normalized active area vs. breakdown voltage) shown in Fig. 5, which presents a clear trend of a reduced normalized active area with increasing breakdown voltage due to its enlarged edge termination [112]. The normalized active area does not consider the difference in die sizes and rated current levels, which inevitably puts larger dies in favor due to the relatively smaller edge termination.

B. SiC Power Modules and Packaging

For high-power electronic applications, power modules are used to integrate multiple semiconductor devices into one single package to increase the current handling capability and minimize parasitics. Most importantly, the design of the power

TABLE II
OVERVIEW OF MV SiC POWER MODULES WITH AVAILABLE DATA OF JUN. 2024 AND EXPANDED FROM LI ET AL.'S [156] WORK

Year	Affiliation	Package	Breakdown voltage (kV)	Output current (A)	Total no. of devices	Module size (mm)	Power density (kVA/cm^2)	Configuration	Power loop inductance (nH)	Switching energy (mJ)	Ref.
2015	Wolfspeed†	–	3.3	180	8 + 8	107 x 62 x 31	35.1	Half bridge	–	45	[157]
2015	Mitsubishi†	–	3.3	1500	16 + 16	–	–	Half bridge	–	1970*	[158]
2017	Wolfspeed†	XHV-7	3.3	500	16	100 x 140 x 40	68.8	Half bridge	10	68	[159]
2018	Mitsubishi†	LV100	3.3	400	–	100 x 140 x 40	91.7	Half bridge	10	251	[125]
2018	Fuji†	–	3.3	200	–	98 x 65 x 21	40.5	Half bridge	–	235	[160]
2018	U. of Nottingham‡	–	3.3	100	4	120 x 61	18.2	Half bridge	24	–	[161]
2019	Hitachi†	nHPD^2	3.3	1000	–	100 x 140 x 38	138	Half bridge	10	1510*	[162]
2020	ABB†	LinPak	3.3	450	40	100 x 140 x 38	61.9	Half bridge	10	210	[163]
2021	Toshiba†	iXPLV	3.3	800	–	100 x 140 x 38	110	Half bridge	12	610*	[164]
2021	U. Texas Austin‡	–	3.6	400	24	–	–	SC	35	–	[165]
2021	Fuji†	HPnC	3.3	750	–	100 x 144 x 40	101	Half bridge	10	540	[166]
2023	Stony Brook U.‡	XHP	3.3	200	8	100 x 140 x 40	27.5	Half bridge	30	–	[167]
2023	U. of Arkansas‡	–	3.3	200	8	104 x 100 x 24	32.4	Half bridge	6.9	25.7	[168]
2023	Wolfspeed†	LM3	3.3	800	–	100 x 140 x 38	110	Half bridge	11	380	[169]
2024	Wolfspeed†	LM3	3.3	770	–	100 x 140 x 44	106	Half bridge	–	–	CAB600M33LM3
2024	Mitsubishi†	LV100	3.3	750	–	100 x 140 x 40	103	Half bridge	–	850*	FMF750DC-66A
2024	Minebea†	nHPD^2	3.3	800	–	100 x 140 x 38	110	Half bridge	10	1340*	MSM800GS33ALT
2014	USCi‡	–	6.5	60	8 + 8	120 x 80	19.5	Half bridge	–	37.8	[131]
2018	Mitsubishi†	HV100	6.5	400	–	100 x 140 x 40	108	Half bridge	–	520*	[170]
2020	Wolfspeed†	XHV-7	6.5	400	–	100 x 140 x 40	108	Half bridge	–	450	[171]
2020	U. Texas Austin‡	–	7.2	60	–	170 x 60 x 35	18.8	SC	–	–	[172]
2020	Nanjing NEDI‡	–	6.5	400	–	130 x 140 x 48	96.3	Half bridge	–	1220	[173]
2023	XJTU‡	–	6.5	25	2	37 x 27 x 3.5	25.4	Half bridge	2.6	–	[174]
2011	Cree†	–	10	120	24 + 12	140 x 190	36.4	Half bridge	25	110	[121]
2016	Wolfspeed†	XHV-6	10	240	18	195 x 125 x 23.5	75	Half bridge	16	–	[175], [176]
2017	Aalborg U.‡	M4x	10	10	2	104 x 59 x 35	6.1	Half bridge	72	25.7	[177], [178]
2018	Virginia Tech‡	–	10	60	6	83 x 68 x 25	39.7	Half bridge	4.4	–	[179], [180]
2020	Wolfspeed†	XHV-9	10	16	2	65 x 125 x 23.5	8.4	Half bridge	–	21	[181]
2020	Aalborg U.‡	M5x	10	80	8	104 x 59 x 35	49.1	Half bridge	21	140	[182]
2013	Cree†	–	15	20	1 + 2	114 x 63	16.9	Single switch	–	–	[122], [141]
2014	Japan AIST‡	–	16	60	4 + 1	65 x 74	69.1	Single switch	–	340	[123], [144]
2016	Cree†	–	24	30	–	–	–	Half bridge	–	–	[183]

‡Academia †Industry *Specified at T_j of 175°C
All values are specified at room temperature unless otherwise specified.

module package should ensure good electrical performance, high reliability, and efficient thermal management. In general, adhering to an industry-standard package footprint and pinout eases the assembly for future system utilization.

MV Si IGBT power modules are currently prevalent in the market; however, the development of MV SiC power modules is gathering significant interest from both industry and academia. An exhaustive list of MV full-SiC power modules, both commercially available and engineering samples, are presented in Table II and ordered in terms of their breakdown voltage and announced year. As apparent from the table, power modules at 3.3 kV have gained significant interest from large industry players and have become commercially available during 2024. Although multiple power modules with breakdown voltages at 6.5 and 10 kV have been announced, the industry players are currently limited to Mitsubishi and Wolfspeed.

Packaging of industrial high-power MV Si IGBT power modules tends to be in standard packages in sizes of 73 × 140 mm, 100 × 140 mm, 130 × 140 mm, and 140 × 190 mm depending on the power level. However, apparent from Table II, a strong tendency toward 100 × 140 mm packages, as the one shown in Fig. 6, for MV SiC MOSFET power modules at 6.5 kV and below is shown from industry. This package size is anticipated to be the future standard package size for high-power electronic applications.

A cross-comparison between the MV SiC power modules in Table II and several commercially available Si/SiC hybrid from Dynex [153], Infineon [154], and Hitachi/Minebea [155]

Fig. 6. Majority of available MV SiC MOSFET power modules use a standard 100 × 140 mm footprint, widely accepted for 3.3 and 6.5 kV Si IGBTs.

has been performed in terms of their static and dynamic performance. The Si/SiC hybrid power modules utilizes Si IGBTs as switching devices and SiC Schottky barrier diodes or junction barrier Schottky diodes as freewheeling diodes.

1) Their static performance (current density versus breakdown voltage) is shown in Fig. 7 with the majority of the power modules utilizing MV SiC MOSFETs or MV Si IGBTs as switching devices. Although the MV SiC IGBTs showed an increased power density compared to SiC MOSFETs on a device-level in Fig. 2, the power density of the two included SiC IGBT modules lies in the same

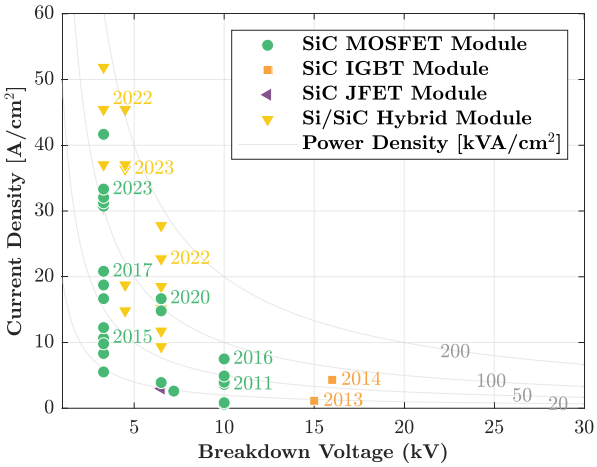

Fig. 7. Static performance of MV SiC and Si/SiC hybrid power modules. Data source: Si/SiC hybrid power modules [153], [154], [155].

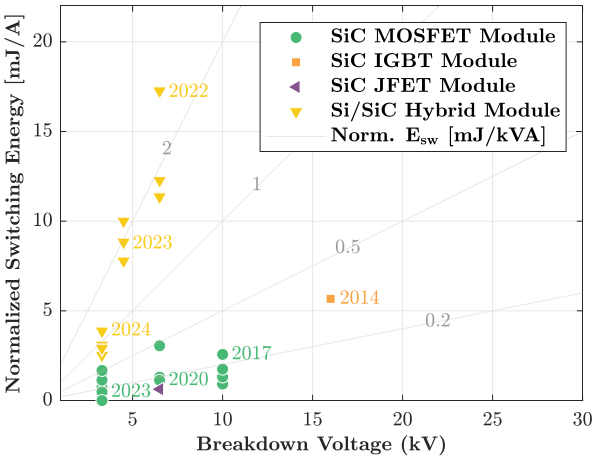

Fig. 8. Switching performance of MV SiC and Si/SiC hybrid power modules. Data source: Si/SiC hybrid power modules [153], [154], [155].

range as the SiC MOSFET ones. With only two MV SiC IGBT samples, conclusions should be carefully drawn; however, a possible reason is the required freewheeling diode, which takes up space within the power module. The Si/SiC hybrid power modules is the closest competitor to the MV SiC MOSFETs in the voltage range from 3.3 to 6.5 kV, which shows a slightly higher power density in the whole voltage range, anticipated to be caused by their improved maturity.

2) Their dynamic performance (normalized switching energy versus breakdown voltage) is shown in Fig. 8 for those MV SiC power modules that have readily available switching energies or waveforms. In addition, switching energies from the commercially available Si/SiC hybrid power modules have been included for comparison. To make a fair comparison throughout the whole voltage range, the included switching energies are collected at 50%–60% of rated breakdown voltage [103] and at approx. its rated forward current. However, the comparison does not consider differences in dv/dt, di/dt, gate resistances, or test setups, which inevitably impacts the accuracy of the comparison. From the comparison, it is evident that full-SiC MOSFET power modules have comparable lower switching energies compared to Si/SiC hybrid power modules in the range of 3.3–6.5 kV, which allows for elevated switching frequencies.

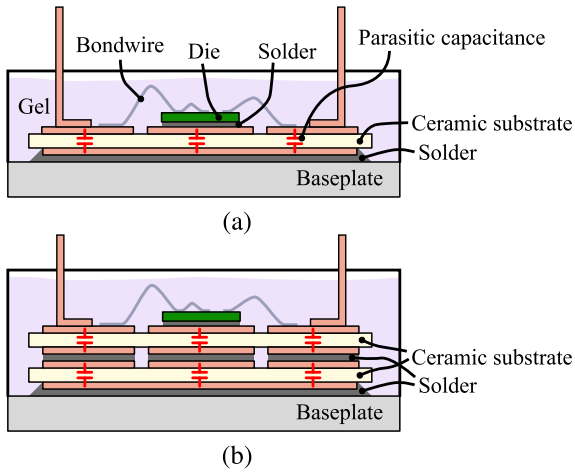

Fig. 9. Cross-section diagram of power modules using (a) conventional structure and (b) double-stacking of DBCs to reduce capacitive coupling.

The commercially available MV SiC power modules listed in Table II predominantly adhere to the conventional packaging structure [184], [185], [186], as shown in Fig. 9(a). In these power modules, the SiC semiconductor devices are attached to the top-side of a direct-bonded copper (DBC) ceramic substrate, and bondwires are used for interconnections to the SiC semiconductor devices. The bottom layer of the DBC is connected to the baseplate, and finally, the insulation of the package is ensured by an encapsulating gel. Besides the electrical performance parameters listed in Table II, the choice of a suitable power module for MV applications also relies on its thermal performance and mechanical reliability, which depends on materials used in substrate, baseplate, attachment layers, and interconnects of the power module.

1) Substrate: Conventional power modules use DBC substrates, a technique that involves the direct bonding of copper to both sides of a ceramic substrate, bypassing the use of supplementary adhesives or brazing materials. The substrate plays a critical role, facilitating not only the electrical connection for semiconductors and power terminals but also providing the thermal path and electric insulation to the baseplate. A popular material for ceramic substrates is alumina (Al_2O_3), which in LV power modules typically has a thickness of 0.25–0.63 mm, whereas, in MV power modules, the thickness of the ceramic can be increased to 1 mm or more to further improve the insulation strength and reduce parasitic capacitances of the module at the cost of increased thermal resistance. To alleviate this drawback, ceramics of aluminum nitride (AlN) can be used instead, as its thermal conductivity is 170 W/(m · K), in comparison with the 24 W/(m · K) of Al_2O_3 [187].

To further reduce the parasitic capacitance, researchers at Virginia Tech, University of Nottingham [179], [180], and

Aalborg University [182] have designed 10kV SiC MOSFET power modules that use stacked DBCs, as shown in Fig. 9(b), effectively series connecting the parasitic capacitances. In addition, using the middle-potential of the stacked DBC mitigates high electric fields, thus improving the insulation strength and partial discharge (PD) inception voltage level.

2) Baseplate: The substrate is generally attached to a baseplate, which serves as the main heat transfer path to the cooling system as well as providing mechanical support. Selection criteria for baseplate materials similarly emphasize high thermal conductivity, but also a coefficient of thermal expansion (CTE) which matches the material of the neighboring parts. Typically, copper is preferred as baseplate material because of its thermal conductivity of 400 W/(m · K); however, with a CTE of 17 ppm/K, copper baseplates do not match well with the low CTE of the AlN ceramic of 4.7 ppm/K, eventually causing failure due to delamination or cracking of the ceramic [188]. Therefore, some power modules use baseplates where SiC powder is embedded into magnesium or aluminum to form MgSiC and AlSiC baseplates, which have CTEs of around 7.0 and 7.4 ppm/K, respectively, but can be configured by changing the mixing ratio of the SiC powder [189], [190]. The drawback of using MgSiC or AlSiC baseplates is a comparatively lower thermal conductivity in the range of 230–240 W/(m · K).

3) Attaching Materials: Criteria for die attachment material selection include high thermal conductivity, low electrical resistance, and a CTE closely aligned with that of the substrate. Solder paste, such as Tin-Lead (SnPb) and Tin-Silver-Copper (SnAgCu), is mainly employed for these attachments, owing to its widespread acceptance in current manufacturing practices. Silver sintering is a notable alternative, offering superior thermal conductivity at 429–459 W/(m · K) compared with 50–70 W/(m· K) of Tin-based solders [191]. Die attachments formed through silver sintering also have melting points greater than 300 °C [192], compared to 217 °C of SnAgCu-solder, and a lower CTE [193] to better match with materials, such as SiC and AlN [194]. Silver sintered joints are also reported to have over 400 times longer fatigue lifetime [195] than Sn-based solder connections under the same thermal cycling conditions. However, its adoption has been limited due to higher costs and more complex manufacturing requirements.

4) Interconnection Method: The internal connection between the top-side of the semiconductor device and the top-side of the DBC plays an important role in power module packaging as it contributes to the power loop inductance, which has been a major concern in LV power modules with high current ratings. Presently, wire bonding techniques are the most widely used method, which utilizes 125–500 μm aluminum wires to establish the internal connections [196]. Despite wire bonding's simplicity and cost-effectiveness, it still suffers from notable drawbacks of substantial parasitic inductance and concerns about its reliability. Wire bond failures at the heel of the wire bond are a common failure mechanism due to the mismatch in CTE between the bonding material and the SiC semiconductor device. The CTE of aluminum is in the range of 21–24 ppm/K and compares to a CTE of 4.7 ppm/K for SiC. To address these challenges, various wire bondless methods have been developed such as ribbon bonding [197], flip chip technology [198], power tap and planar interconnection [199], direct pressed die [200], vertical copper pins [201], and copper clips [184]; however, currently limited to LV power modules.

III. MV Applications

Several overview papers have already been published in the literature related to the applicability of the SiC technology [103], [202], [203], [204]; however, these overview papers mainly focus on LV applications. Well-established overview papers related to MV applications are limited to Ji et al.'s [93] work, in which only solid-state transformers (SSTs), motor drives, and grid-connected converters utilized in conventional grid applications are discussed, and to Han et al.'s [108] work, in which SST, conventional grid, and other applications enabled by MV SiC IGBTs are discussed. The applicability of the MV SiC technology is further discussed for certain specific applications, i.e., distribution grids [95] and SSTs [205].

The interest in exploring the applicability of the MV SiC technology started during the last decade; however, the MV SiC technology has experienced significant advancements in recent years, not only with the introduction of the first commercially available MV SiC semiconductor devices but also from the increasing interest from industry and academia to design high-performance power modules, which paves the way for full exploration of the applicability of the emerging technology. Therefore, this section further reviews some typical high-power electronic applications individually and highlights the unique benefits of utilizing the MV SiC technology. The section is organized in three parts covering renewable energy generation, grid distribution, and consumption.

A. Renewable Energy Generation

The MV SiC technology has the potential to revolutionize the generating sources of renewable energy by transitioning from an LV to MV architecture and adopting new converter typologies enabled by the MV SiC technology to improve power capabilities and material footprint. With PVs and wind turbines being major sources of renewable energy, research pertaining to these applications has gained an increasing interest in recent years from industry and academia.

a) Photovoltaic: Solar energy is currently among the cheapest sources of renewable energy [2]. Solar energy is harvested from PV panels varying from single units on household rooftops to large-scale utility plants in rural areas. As this article focuses on high-power electronic applications, the focus of this section will be targeted at large-scale utility plants in the size of multimegawatts. Nowadays, the conventional architecture of large-scale utility plants, from solar panel to grid connection, includes multiple solar panels, several string converters, a central inverter, and a low-frequency LV to MV service transformer connected to the grid [206], [207], [208]. The string converter, a dc/dc converter, follows typically a maximum power point tracking algorithm and feeds into a common dc-bus of 1 kV or less [208], [209]. Then, the large central inverter connects the common dc-bus to the MV grid through the LV to MV service

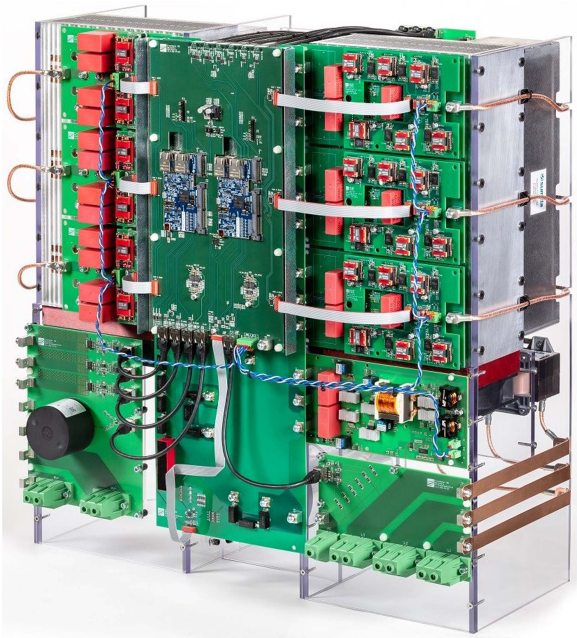

Fig. 10. Fraunhofer ISE 3.3 kV, 250 kVA string inverter for PVs [212], [213].

transformer and controls the power flow from the PV plant to the grid.

Well-renowned manufacturers of large-scale central inverters for PV applications are Ingeteam [63], TMEIC [65], Sungrow [66], ABB [67], SMA Solar Technology [68], Power Electronics [70], and Siemens [75] to name a few. Several of the companies have released central inverters with an increased dc-link voltage of 1.5 kV, enabled by three-level typologies and LV IGBTs, to benefit from the increased voltage level [63], [65], [67], [69], [75], which include copper and switchgear savings as well as improved performance at wider temperatures and irradiance ranges [209]. In addition, recent industry-driven projects on MV string converters and/or central inverters [210], [211], [212], [213] investigate the potential of MV SST-based typologies enabled by SiC MOSFETs, especially in [212] and [213], in which the world's first MV string converter based on 3.3 kV SiC MOSFETs is presented and shown in Fig. 10, which results in enormous material savings for passive components and cables [213].

The increasing interest in the MV SiC technology in relation to string converters and central inverters for large-scale utility plants is not only given by industry but also academia [214]. Overview papers of research activities related to MV central inverters enabled by series connected multilevel typologies and LV IGBTs are discussed in detail in [207] and[208], highlighting an increasing interest in replacing the bulky, low-frequency service transformer with MV SST-based typologies to reduce cost, weight, volume, and losses. Apart from the overview papers, several research institutes have published simulation studies [215], [216], [217], [218] and experimental validations [219] for MV string converters enabled by MV SiC MOSFETs. Further, examples of MV SST-based typologies specifically targeted at large-scale PV applications enabled by LV SiC MOSFETs are given in [220] and [221].

b) Wind Turbine: Wind energy is considered one of the main renewable energy sources paramount for the green transition [3]. To meet the political agendas and demands of increased wind capacity toward 2030 [222], the power ratings of the wind turbines are continuously growing as visualized from the trend of Fig. 1. Large-scale wind turbines for offshore applications were in the last decade limited to a few European companies namely Vestas Wind Systems (VWS) [77] and Siemens Gamesa Renewable Energy [83] together with some minor pioneering companies. However, with non-European wind turbine manufacturers, such as General Electric (GE) [84], MingYang Smart Energy [82], Goldwind [223], Haizhuang Windpower, [89] and Dongfang Electric Corporation (DEC) [78] penetrating the global market around 2020, the sizes of turbines has grown rapidly, with the largest offshore turbines reaching up to 18 MW in power rating [89] and even projected to reach 22 MW already in 2025 [90].

The conventional solutions adopted by the European wind turbine industry previously relied on LV converters based on Si IGBTs operated at a line voltage of 690 V; however, the newer releases from suppliers and manufacturers, such as GE [84], DEC [78], ABB [224], and Ingeteam [225], presents MV converters utilizing the Si IGCT-technology. According to ABB, the benefits of the MV solutions for wind turbines include; reduced current magnitudes, easier integration of converters, less number of, and reduced weight, of cables, a more compact converter footprint, and in general reduced weight of the converter in comparison to the conventional LV design [226]. Among others, these motivations have led VWS to investigate the cost-benefit of the MV SiC converters in comparison to LV and MV Si converters by evaluating the levelized cost of energy (LCoE) [227]. From the cost-benefit analysis, the MV solutions are found to offer benefits in comparison to the LV solutions, such as reduced initial capital investment for the converter and transformer down-tower solutions. However, due to the increased component cost and poor maturity of MV SiC devices, the total LCoE gain is highest for the down-tower solution utilizing the MV Si devices. This corresponds well with the trend from the state-of-the-art commercial solutions where the Si IGCT technology is used. To the best of our knowledge commercial wind turbine applications employing MV SiC converters do not yet exist.

In academia, the concept of MV wind turbines has likewise been under investigation. However, the majority of these research studies are limited to either simulations or analytical models, and thus only a few provide experimental demonstrations of MV SiC power stacks suitable for high-power wind turbines. The state-of-the-art typologies proposed in the literature, applying the MV SiC technology for wind turbine applications, can be categorized as follows. 1) Two- and three-level typologies utilizing the MV SiC semiconductor devices for the wind turbine generator-side and line-side direct drive ac/dc–dc/ac converters [228], [229], [230], [231], [232]. 2) Multilevel typologies utilizing the MV SiC semiconductor devices in dc/dc converters for offshore MVDC collection [233], [234].

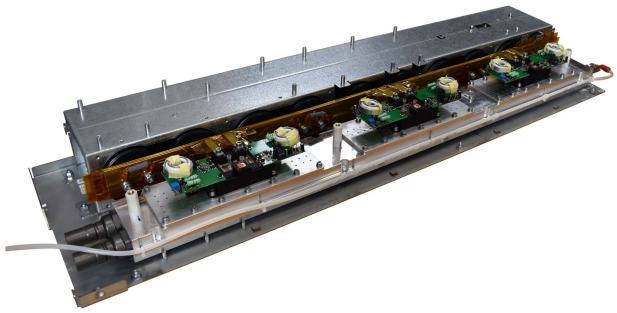

Fig. 11. Aalborg University demonstrates 10 kV SiC MOSFET power stack for wind turbine applications rated at 4.16 kV, 50 kVA, and 5 kHz [231].

The efficiencies for the two- and three-level typologies for the generator-side direct drive converters are simulated and compared in [228] and[229] for both 3.3 and 6.5 kV Si and SiC semiconductor devices. The general trend shows an increased efficiency for the SiC-based typologies in comparison to the Si-based ones, especially at higher switching frequencies. However, the level of detail provided for the simulation models is not comprehensive in terms of device loss characterization, thermal modeling and temperature dependency, and exclusion of conduction losses, thus emphasizing the need for more thorough loss modeling of MV SiC semiconductor devices for wind turbine applications and in general. In Erdman et al.'s [230] work, a 4.5 kV three-level NPC typology for a line-side direct drive wind turbine converter at 3.3 kV grid voltage has been experimentally proven. A full load converter efficiency of above 98% is demonstrated for 4.5 kV Si IGBT power modules, whereas an efficiency of above 98.5% is achieved for 4.5 kV Si/SiC hybrid power modules at 1 kHz. In comparison, a full-SiC two-level generator-side converter utilizing 10 kV SiC MOSFET devices, as shown in Fig. 11, has been proposed and developed in [231], [232], and [235] and was experimentally demonstrated at 5 kHz to have an efficiency of more than 99% at partial load.

In the case of multilevel dc/dc typologies for MVDC collection, the 15 kV SiC MOSFETs and 13 kV SiC IGBTs are compared with the use of analytical models in Chen et al.'s [233] work for the following cascaded multilevel typologies.

1) The hybrid boost and buck-boost converter.
2) The resonant stepup converter.
3) The resonant switched capacitor converter.

The analysis shows that between 580 and 4600 semiconductor devices are needed, depending on the chosen topology, to achieve 40 kV MVDC and that the resonant switched capacitor converter utilizing 13 kV SiC IGBTs and 15 kV SiC diodes is superior to the other typologies in terms of efficiency. In Lagier et al.'s [234] work, the dc/dc converter typologies for an MVDC to HVDC conversion are compared in a simulation study, utilizing the 3.3 kV SiC MOSFETs and Si IGBTs as well as 10 kV SiC mosfets. The typologies under investigation are as follows.

1) Cascaded dual active bridge (DAB) converter.
2) Cascaded series resonant converter (SRC).
3) The MMC.

The analysis shows that between 2300 and 8600 semiconductor devices are needed, depending on the topology, to realize a dc/dc stepup converter from 40 to 320 kV. In addition, it is found that the MMC typology achieved the highest efficiency in the range of 99.6%–99.8% in the midload range from 50–350 MW, whereas in the higher loading range from 350–600 MW, the cascaded dc/dc converters achieved the highest efficiency between 99.4 and 99.6%. In general, the 3.3 kV SiC MOSFETs achieved better performance in terms of efficiency compared to the 10 kV SiC MOSFETs independent of the chosen typology.

B. Grid Modernization

The growing emphasis on reducing carbon footprint due to climate change has led to the evolution of the conventional electric grid into a two-way distributed power flow system comprising power converters. At MV, these converters find application in static synchronous compensators, active filters, bi-directional power converters for grid-integration of renewables and energy storage, EV charging, and power distribution using SSTs [109].

The existing design of MV high-power converters for the distribution grid relies on high-order multilevel converter typologies, where LV, typically, 1.2 or 1.7 kV Si IGBTs are used [236], [237]. Emerging SiC MOSFETs and SiC IGBTs show great potential for simplifying converter typologies, reducing control and design complexity, and improving overall efficiency [238], [239], [240]. First, due to the higher blocking voltage, the need for a series connection of LV devices is eradicated. The series connection has a demerit of control complexity and the need for balancing and snubber circuits for static and dynamic voltage balancing, which increases the semiconductor losses [241], [242]. Second, Si semiconductor devices, compared with SiC ones, have limited switching capability, leading to higher switching losses. Therefore, paralleled converters and bulky passive filters are required for filtering to ensure grid compliance [238]. In contrast, with a single MV SiC semiconductor device coupled with faster switching capability, the need for complex typologies and large passive filters can be eliminated. The typology and filter simplification benefits are promising for lowering cost and increasing power density, efficiency, and reliability. Finally, the fast-switching capability of MV SiC semiconductor devices also allows the development of power converters with faster dynamic response and control bandwidth [95], [243].

Several works in academia have explored utilizing MV SiC semiconductor devices for the conventional grid [181], [238], [244], [245], [246], [247], [248], [249], [250]. The primary research focus has been on lowering control complexity by employing simpler converter typologies and addressing challenges related to the design of MV-rated auxiliary components such as gate drivers and sensors.

For instance, in [238], [249], and [250], a 100 kVA five-level MMC or flying capacitor (FC) converter is developed using discrete 10 kV SiC MOSFETs to interface a microgrid with 13.8 kV ac of distribution voltage at 10–15 kHz switching frequency. Due to the high breakdown voltage of SiC MOSFETs, a five-level converter typology is adopted to achieve the desired 25 kV dc bus voltage and 13.8 kV ac voltage using four (sub)modules.

In [244] and [245], a two-level active front end (AFE) converter rated at a dc voltage of 7.2 kV, 35 kW, and 10 kHz is

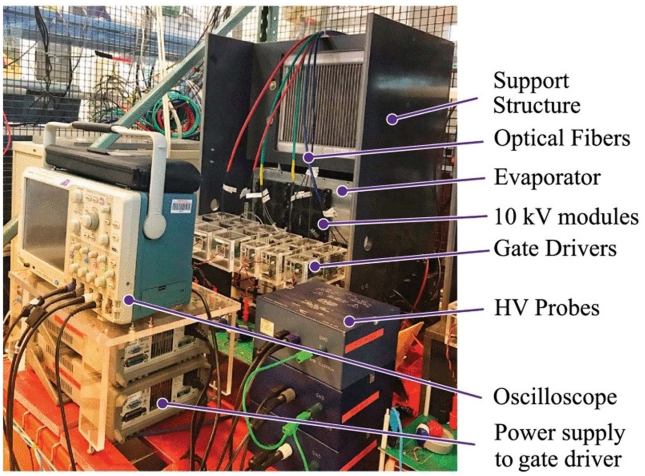

Fig. 12. North Carolina State University demonstrating an MV power block for SST using 10 kV SiC MOSFETs rated at 35 kW and 10 kHz [244].

developed using 10 kV SiC MOSFET modules in the XHV-6 package, as shown in Fig. 12, with a peak efficiency of 95.5%. The cost-share of 10 kV SiC MOSFETs is exorbitant and is reported as 81% of the total converter cost. However, it should be noted that 10 kV SiC MOSFETs, at present, are still in the nascent stage of development, leading to high costs.

Similarly, in [246] and [247], 10 kV SiC MOSFETs and 15 kV SiC IGBTs are compared for MV transformerless intelligent power substation, a three-phase typology for SST capable of providing grid-support functions for a 13.8 kV distribution grid. For the AFE converter, both SiC MOSFET- and SiC IGBT-based rectifiers show high efficiency up to 10 kHz switching frequency owing to their fast-switching capability. The SiC IGBT provides a slightly higher loss than the SiC MOSFET-based converter, which is shown to be reversed for higher power levels ($>$1 MVA) due to lower conduction loss. Further, due to higher switching frequencies above 3 kHz, the maximum filtering requirement is dropped from 0.1–0.15 pu inductance using GTOs to as low as 0.05 pu for SiC semiconductor devices. The reduction in filter size is beneficial in achieving faster dynamic response [246].

In addition, in Ji et al.'s [248] work, a 100 kVA five-level MMC enabled by 10 kV SiC MOSFETs is presented with the potential of direct connection to the 13.8 kV grid with a dc-link voltage of 25 kV. The converter obtains an estimated efficiency of 99.3% and a power density of 0.24 kW/L at 10 kHz.

Further, an 11 kV ac, 16 kV dc, 200 kW, two-level inverter building block is developed in Ravi et al.'s [181] work, showing an projected efficiency of 99% and power density of 2.75 kW/L at 10 kHz. A half-bridge 10 kV SiC power module in the XHV-9 package is used for each switching position, providing a total of 20 kV blocking voltage. Due to the series connection, a voltage balancing issue arises, which is resolved by using an active gate driver with timing-based voltage balancing and short-circuit protection capability. Moreover, field grading is employed for the planar PCB bus to prevent corona and PD.

General examples and experimental validations of MV SSTs enabled by 3.3–15 kV SiC MOSFETs targeted at grid applications are given in [251], [252], [253], [254], [255], [256], [257], [258], and [259]. In addition, Doncker [260] presented a size comparison of an MV low-frequency service transformer and an MV medium frequency transformer intended for SST use, as shown in Fig. 13, from which a distinct size and weight reduction is achieved.

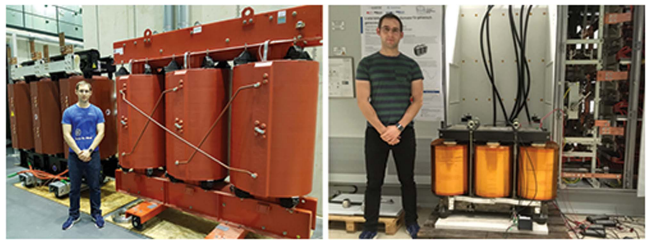

Fig. 13. E.ON ERC—PGS at RWTH Aachen University size comparison of two three-phase, dry-type low and medium frequency transformers. *Left:* 4.5 MVA, 50 Hz, 11.500 kg. *Right:* 5 MVA, 1 kHz, 675 kg [260].

In summary, the MV SiC technology shows excellent potential in developing compact high-power converters with fast dynamic response to support the future grid. Nevertheless, the high device cost of MV SiC semiconductor devices and power modules, attributed to its early development stage, and the design complexities associated with auxiliary components pose significant challenges.

C. Consumption

Electrification of society and the green transition elevates the consumption of renewable energy in sectors of EV charging, future computing infrastructure, electrolyzers, and motor drives to limit the environmental impacts. Currently, the MV SiC technology has not penetrated the consumption sector but presents several benefits compared to the state-of-the-art solutions.

1) EV Charging: Today, EVs are not only limited to scooters and cars, but also include large vehicles, such as electric buses, trucks, vessels, and aircraft. Electrification of the transport industry, both road and nonroad vehicles, has become extremely popular in recent years and the term "EV" has become universally known. The discussion on EVs is twofold, as EVs and charging of EVs go hand in hand, and for high-power electronic applications, the topic of interest is EV charging, and more specifically the dc fast charger above hundreds of kilowatts. The EV charging requirements among the different EVs differ significantly due to the difference in battery capacity and charging pattern, which may range from tens of kWh for electric cars to single-digit MWh for electric vessels [18]. A general discussion covering both types of EV charging can become a challenge, and therefore, this section is divided into two.

a) Charging of light transport: The EV charging market was pioneered by Tesla during the last decade; however, multiple manufacturers have ever since entered the market, such as ABB [8], Alpitronics [9], Siemens [10], SK Signet [14], and Tritium [15] to name a few. Previously, all of the commercially available dc fast chargers adhered to the same architecture: a low-frequency service transformer to convert the MV grid connection to an LV ac, then an ac/dc converter to rectify the ac

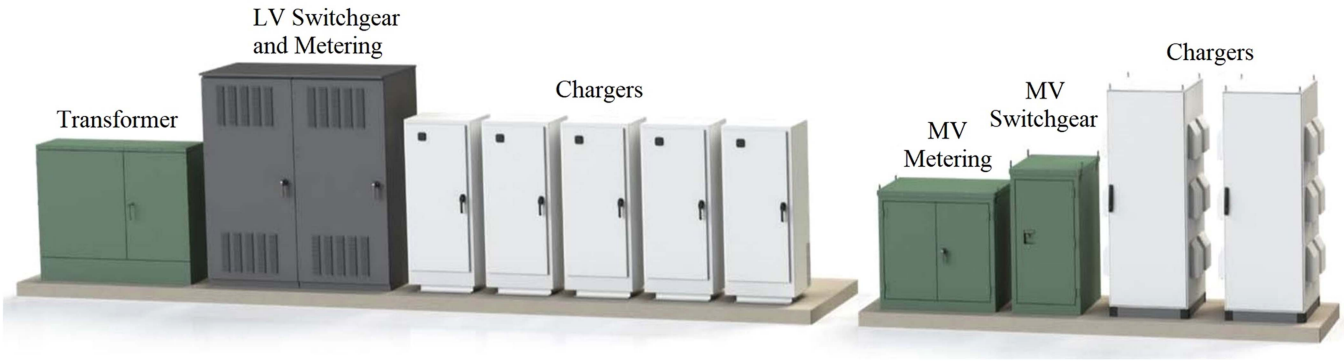

Fig. 14. North Carolina State University comparison of state-of-the-art DC fast charger and MV SST-based solution at a rated power of 675 kW [268].

voltage into an intermediate dc voltage, and at last, a dc/dc converter to interface the battery of the EV [261]. However, recent industry-driven projects, such as [262], [263], [264], and [265], investigate the possibilities of transitioning from the state-of-the-art architecture into a more flexible and scalable SST-based typology enabled by SiC MOSFETs. In both [262] and [263], an MV grid connection of 13.2 kV is under investigation and to comply with the blocking voltage, a series connection of either neutral point clamped (NPC) or FC typologies enabled by LV SiC MOSFETs are being implemented. In both cases, the series connected multilevel converters could be directly replaced by a single two- or three-level typology enabled by the MV SiC technology, which would simplify the converter design significantly.

There exist several academic overview papers in the literature discussing in detail the recent trends and advancements for EV charging [266], [267], [268], [269], [270], [271]. From the overview papers, it is apparent that academia supports the transition from state-of-the-art architectures into SST-based solutions connected directly to the MV grid. The benefits of MV SST-based converters include but are not limited to reduced system size, improved conversion efficiency, more power per footprint, and reduced installation cost [266], [267], [268], [269]. In Tu et al.'s [268] work, the state-of-the-art dc fast charger (Tesla Supercharger [7]) is compared with the MV SST-based solution in terms of system size and power per footprint, as shown in Fig. 14. In both [268] and [269], the use of MV SiC technology, including both SiC MOSFETs and SiC IGBTs, is discussed and highlights that if an MV grid connection can be achieved without any series connection on power module- or converter-level, the complexity of the system significantly reduces. A preliminary design study of a 350 kW MV EV charger, enabled by 10 kV SiC MOSFETs, is presented in Liang et al.'s [272] work and shown in Fig. 15, showing an estimated efficiency exceeding 98% and power density of 1.6 kW/L. Additional examples of MV SST-based typologies enabled by MV SiC MOSFETs targeted at EV charger applications are [273] and [274].

Several independent research institutes highlight the MV SST-based typologies to be particularly suitable for urban areas where space is limited [266], [267], [268] as they enable better size utilization and more compact designs.

Several dc fast charging connectors are currently on the existing market, including CHAdeMO, CCS-1, CCS-2, GB/T, and

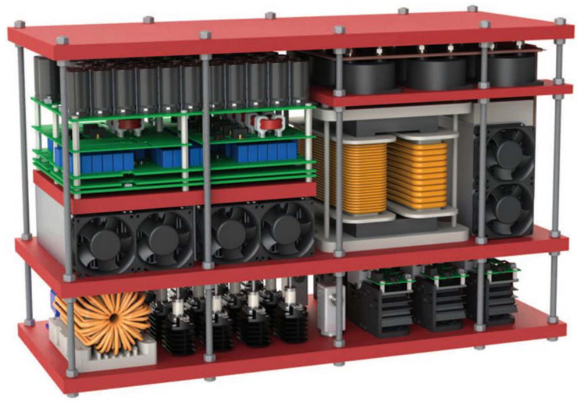

Fig. 15. North Carolina State University 3-D rendering of one phase of the 350 kW EV fast charger enabled by 10 kV SiC MOSFET rated at 12.47 kV grid voltage and operated at 10–25 kHz [272].

Tesla Supercharger [270], which ranges from 480–1000 V in maximum output voltage at a maximum current of 400–800 A, limiting the power to less than 500 kW. However, a new standard charging connection intended for large battery EVs, the megawatt charging system, has emerged with an extraordinary elevated power capability at 3.75 MW (1250 V and 3000 A) to reduce the charging time. Recently, Siemens achieved a milestone by demonstrating a momentary charging capacity of 1 MW at 806 V and 1.24 kA [275].

b) Charging of heavy transport: The market for charging large vessels and aircraft is still a niche market but an important step toward zero-emission sea and air transport. According to Transport and Environment [276], heavy transport within shipping and aviation sectors is undoubtedly dominated by electrofuels, based on green hydrogen, in the coming decades; however, for certain specific tasks or routes, fully electric vessels and aircraft may be the most suitable solution. In the last decade, several industry-driven projects of fully electric vessels [18] and aircraft [277], [278], [279] have been carried out.

Large charging stations for electric vessels adhere to the same architecture as the one described for charging of light transport except for a local onshore energy storage system being integrated into the charging station to limit the power drawn from the grid during charging [18]. A highly discussed topic related to

large charging stations for electric vessels is the shore-to-ship interface, which currently is transitioning from a manual to an autonomous plug system due to the time-consumption, safety, and size of charging cable(s). A potential solution to reduce the cable size would be to establish an MV shore-to-ship charging connection; however, this would require the MV technology to further mature for this to become viable.

Charging stations for electric aircraft differ significantly compared to the former ones, as mobile charging units (MCUs) with LV battery packs are of high interest [277], [278], which can be towed on the apron of the airport. The chargers are operated at LV to comply with the battery voltage; however, research within MV batteries for the aviation sector is under investigation due to their improved energy density and weight [280], [281], which inevitably requires MV PECs to convert the energy from the charging unit to the battery of the electric aircraft. An example of such a MCU was presented by Pratt and Whitney Canada earlier in 2024 with a charging capacity of 280 kW at 1500 V [282].

2) Future Computing Infrastructure: Power demand and energy consumption in data centers have increased significantly in recent years, with extensive development and advancement in cloud computing and Internet of Things. The core component in data centers is the server, which operates at LVDC with high current levels [283], [284].

Traditionally, the power distribution network in data centers is operated at LVAC or LVDC. For both types of power distribution networks, the grid voltage is stepped down from MVAC (4.16–35 kV) to LVAC (208–480 V) through a low-frequency service transformer, which is then either directly distributed among the servers of the data center with localized rectifiers or fed through a centralized rectification stage to generate an LVDC to be distributed among the servers [285]. For rectification, a power factor correction is employed to lower the reactive power flow; however, for MW-scale data centers, both approaches result in exorbitant currents through the power distribution network, lowering efficiency, and increasing busbar/cabling costs.

To address this, a new architecture has gained popularity in academia [286], [287], which uses MVAC as the distribution voltage inside the data center in contrast to LVAC or LVDC. For each server room, a dedicated modular MVAC to LVDC power converter, referred to as an SST, is utilized to convert the MVAC grid voltage to the required LVDC of the servers. As a result, the bulky low-frequency service transformer is eliminated as the SST utilizes a smaller medium frequency transformer. In general, the conversion from MVAC to LVDC comprises two conversion stages, i.e., a ac–dc and a dc–dc conversion stage. The cascaded H-bridge (CHB) multilevel typology is predominantly employed for the ac–dc conversion stage to reach the desired MV (4.16–35 kV), whereas isolated typologies, such as DAB and LLC resonant converters, are employed as the dc–dc conversion stage for each H-bridge of the ac–dc stage [287]. Therefore, the system configuration normally follows an input series, output parallel (ISOP) to comply with the large input voltage and large output current [288].

A performance benefit of the SiC technology compared to its Si-counterparts is their high switching frequency capabilities, which enables higher power density, crucial for data centers where space is a constraint. The existing development of SSTs for data centers using SiC MOSFETs is based on 1.2 kV MOSFETs, owing to their mature fabrication process and wide commercial availability; however, multiple 1.2 kV MOSFETs are connected in series to meet the required blocking voltage [286]. The series connection requires additional gate drivers and voltage balancing circuits [289], which add more complexity to the design. Further, it also brings concerns about reliability due to unbalanced stress and degradation of semiconductor devices due to manufacturing tolerances.

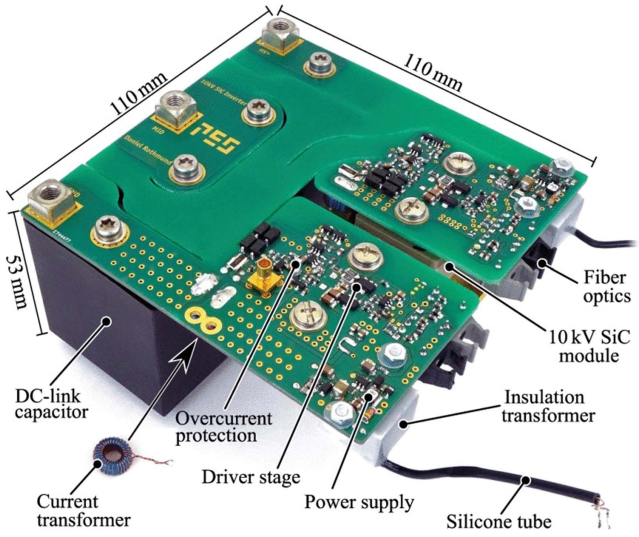

Fig. 16. ETH Zurich 10 kV SiC MOSFET half-bridge board for 25 kW, 48 kHz, 7 kV/400 V DC transformer for data centers [287].

The emergence of MV SiC semiconductor devices enables the development of SSTs with high blocking voltage on the ac side with a comparatively lower number of semiconductor devices in series. For instance, in Rothmund et al.'s [287] work, a 25 kW, 48 kHz, 7 kV–400 V SST is developed using 10 kV SiC MOSFETs as shown in Fig. 16. A single H-bridge is employed as an AFE rectifier for the ac–dc conversion stage and a single isolated LLC resonant converter is utilized for the dc–dc conversion stage. Due to the 10 kV breakdown voltage of the SiC MOSFET, only a single device per switch position is used, requiring only one gate driver per position. As a result, the dc–dc stage is quoted to achieve 3.8 kW/L power density at an efficiency of 99.0% [287]. In comparison, an isolated LLC resonant converter enabled by 6.5 kV SiC MOSFETs are characterized and designed in Du et al.'s [290] work at 25 kW, 50 kHz, 3 kV–540 V achieving a power density of 5.0 kW/L. In Acharya et al.'s [289] work, a 20–11 kV DAB converter is developed using 10 kV SiC MOSFETs as building blocks for a 80–11 kV power conversion in which four DAB converter blocks are connected in an ISOP configuration. For the DAB module, three devices on the primary side and two on the secondary side are connected in series to achieve the required blocking voltage. The proposed converter is intended to supply data centers directly from a multiterminal dc grid, which has a lower capital cost and losses than equivalent MVAC systems [289].

In summary, the power demand for future data centers is expected to increase exponentially and the need for highly efficient and reliable power conversion networks is at an all-time high. Transforming from LVAC and LVDC to MVAC or MVDC power distribution networks inside the data center is a viable approach to reduce transmission losses and heightening efficiency. However, to achieve this, power-dense and efficient power converters are required to directly step down the MVAC or MVDC to the required LVDC at the servers. A promising technology to support this transformation is the MV SiC technology, which features improved power density and system-level reliability by reducing the number of devices connected in series.

3) Electrolyzers: Although the electrochemical process of electrolysis has been known since the middle of the 1800s, the technology has seen an increased interest in recent years due to the green transition. Electrolysis is an essential technology within the green transition, which can contribute to large CO_2 reductions in some of the predominant emission sectors, such as energy, fertilizer, and chemical industries as well as heavy transportation of trucks, buses, vessels, and aircraft. Several well-renowned companies within heavy industries (i.e., steel, machines, power electronics, and chemistry) have entered the electrolysis market, each one having its own strategy to achieve the most efficient large-scale electrolyzer plant. Plug Power [48], H-TEC Systems [49], Green Hydrogen Systems [51], McPhy [56], and Siemens Energy [57] use minor electrolyzer stacks of 1 MW or less; Nel Hydrogen [44], Cummins [46], and ITM Power [55] use medium electrolyzer stacks between 1 and 5 MW; and John Cockerill [45], Asahi Kasei [50], Stargate Hydrogen [52], Sunfire [53], and ThyssenKrupp [54] use large electrolyzer stacks of above 5 MW to form a large-scale electrolyzer plant, which highly impacts the PEC required to supply the electrolyzer stack(s).

Even though the above-mentioned companies present different strategies on a stack-level, they agree upon the architecture for the power supply unit. In general, the state-of-the-art power supply unit connects to the MV grid through an MV/LV low-frequency service transformer followed by a multipulse rectification stage enabled by high-power diodes, thyristors, or Si IGBTs to connect the electrolyzer stacks [291]. In academia, advanced MV SST-based typologies are being discussed as they theoretically improve power quality, efficiency, and controllability as well as exploit the opportunity of avoiding the bulky service transformer [292]. A key component in MV SST-based typologies is the medium frequency transformer, providing voltage conversion and galvanic isolation. In general, the medium frequency transformer design becomes a tradeoff between its power rating and frequency, as these highly impact the power density, thermal performance, and size [293]. A 25 MVA, 400 Hz, 25.4 kV/560 V transformer intended for electrolyzers has been simulated in COMSOL [293], showing a weight reduction of 70% compared to a commercially available service transformer at an approx. size of 3 m^3 and an efficiency of 98.9%. The current research pertaining to electrolyzers enabled by the MV SiC technology is limited; however, in Yan et al.'s [294] work, a 20 kW, 50 kHz MV SST-based dc/dc converter targeted at electrolyzers has been designed to convert a 6 kV dc to 500 V dc to comply with the electrolyzer stack voltage, while in Zhao et al.'s [295] work, a 500 kW grid integration study of an AFE and SST-based dc–dc converter enabled by 10 kV SiC MOSFETs operated at 4 kHz and connected to a 4.16 kV grid has been carried out at different grid conditions (short circuit ratio and voltage deviation).

4) Motor Drives: Industrial motor drives are widely used in various applications, including pumps, fans, compressors, conveyors, etc. [59], which requires efficient conversion and high reliability. MV motor drives are an efficient and cost-effective solution for operating high-power motors and generators [296]. At which power level, MV motor drives become a better economic choice than LV motor drives varies among the large manufacturers of motor drive solutions. Siemens [59] states a minimum power level of 1000 horsepower (HP) while TEIMC GE's [58] range falls between 500 and 1500 HP [297]. The most common working voltage of MV drives are 2.3, 3.3, 4.16, 6.9, 11, and 13.8 kV [298].

The main benefit of MV over LV motor drives is the critically lower inrush and steady-state current for a given mechanical power output. This results in lower cable losses and allows for comparatively thinner cables, which eases the placement and routing of cables from inverter to motor [299]. Further, MV motor drives rated at the utility distribution voltage do not require a low-frequency service transformer to step down the distribution voltage to LV, which inevitably saves space and cost. These drives normally use an AFE rectifier typology to directly convert the MVAC from the grid to an MVDC [300].

The existing commercial MV motor drive designs are dominated by Si IGBTs and thyristor solutions owing to their mature fabrication process, high current ratings, and low conduction losses [301], [302]. Typical converter typologies for commercial motor drives include NPC, active NPC (ANPC), CHB, and MMC as the most mature multilevel typologies. From a voltage level perspective, multilevel typologies enabled by Si IGBTs, such as the three-level NPC and the five-level ANPC typologies are preferred for voltages up to around 7 kV, whereas the high-order MMC typology is preferred for even higher voltage levels. In Bartos's [297] work, an NPC typology is used to design a motor drive for a 4 kV, 4.16 MVA motor, while in Adamowicz and Szewczyk's [303] work, a seven-level CHB typology enabled by 1.2 kV SiC MOSFETs is designed for a 3 kV, 335 kVA railway traction system. Similarly, in the commercial space, the five-level ANPC typology is employed in ABB ACS2000 series motor drives for voltages up to 6.9 kV [300].

Emerging MV SiC semiconductor devices with fast-switching capability (high dv/dt and di/dt) show great potential in enhancing the efficiency and power density of MV motor drives [304]. However, commercial MV drives currently do not employ the SiC technology, primarily due to the limited commercial availability of MV SiC devices [305]. Nevertheless, recent research efforts in academia have focused on exploring the feasibility and performance benefits of adopting MV SiC semiconductor devices in common typologies for commercial drives. For instance, in Marzoughi et al.'s [298] work, a comparison of the performance of 1.7 and 3.3 kV Si IGBTs and 3.3 kV MOSFETs is carried out for CHB, MMC, and five-level ANPC

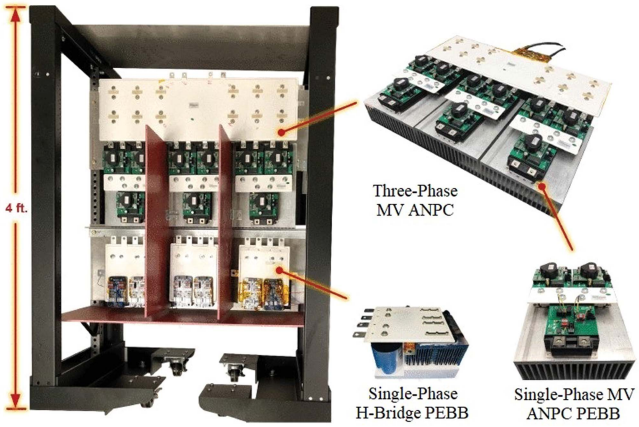

Fig. 17. University of Arkansas design of 7 kV, 1 MVA, 20 kHz Si/SiC hybrid multilevel motor drive for aircraft propulsion [311].

typologies in the range of 4.16–13.8 kV from which conclusions show that the SiC MOSFETs provide high power density for the five-level ANPC typology, while for MMC and CHB, the effect first becomes visible at higher voltages. In Kokkonda et al.'s [306] work, 6.5 kV SiC MOSFETs are demonstrated for a 2.3 kV, 100 kVA motor drive operated at 12.5 kHz, while a series connected of two 3.3 kV SiC MOSFETs is demonstrated at 10 kHz using an auxiliary resonant commutated pole converter for the same motor drive in Kokkonda and Bhattacharya's [307] work showing better electrical performance at lower cost. A 300 kW, 15 kHz DAB enabled by 3.3 kV SiC MOSFET is designed for railway traction applications in Fortes et al.'s [308] work. In addition, the following industry-driven project [309], [310] intends to demonstrate a 4.16 kV, 5 kHz motor drive above 1 MVA utilizing two-level 10 kV SiC MOSFETs in the XHV-6 package from Wolfspeed, targeting to increase the power density from 0.22 to 0.66 kW/L.

Despite their potential performance benefits, the fast-switching capability of SiC MOSFETs brings concerns about exacerbated side effects, such as electromagnetic interference (EMI), bearing currents, and PD. Therefore, another growing research trend in academia is on exploring multilevel typologies, providing optimal performance while minimizing side effects [311], [312], [313]. In Diao et al.'s [311] work and shown in Fig. 17, a seven-level MV Si/SiC hybrid multilevel motor drive for aircraft propulsion is proposed for MW-scale. The typology offers higher power efficiency and reduced harmonic and common mode voltage compared to the widely used IGBT-based ANPC converters. A quasimultilevel converter is proposed in Diab and Yuan's [312] work, to mitigate the overvoltage oscillations at the motor terminals in motor drive applications that require connection cables between the inverter and motor. The efficiency of the typology is validated by simulations for 10 kV SiC MOSFETs. Likewise, in Zhang et al.'s [313] work, an active wave reflected wave canceller is proposed for the widely adopted ANPC typology to mitigate overvoltage and PD in motor windings.

Overall, transitioning to the MV SiC technology is promising for developing the next generation of power-dense and efficient MV motor drives. However, exacerbation of underlying side effects due to the fast-switching of SiC MOSFETs remains a key challenge.

D. Summary

The MV SiC technology has experienced significant advancements in recent years, directly impacting the applications in which they are being deployed. Multiple benefits of utilizing the MV SiC technology are common among several applications, while others are unique to some.

The increased breakdown voltage of the MV SiC semiconductor devices is the most discussed benefit across all applications as it allows for simplified system-level designs and direct use of low-level typologies, which reduce control complexity and enhance system reliability. In addition, the improved switching performance of especially the SiC MOSFETs is also heavenly discussed for all applications as it allows for elevated switching frequencies, which has been demonstrated up to 50 kHz. The elevated switching frequencies lead to improved power densities by reducing the size and weight of passive components and cables in applications, such as wind turbines, charging of EVs, and data centers, where size and weight are constraints. In a combination of the increased breakdown voltage and elevated switching frequency, the LV to MV SSTs have gained increased research popularity for PV, charging of EV, and data center applications, where either the generation or consumption is dc. An attractive benefit of the LV to MV SSTs is their ability to replace the traditional low-frequency service transformers used to interface the grid in high-power applications with a smaller medium frequency transformer inside the SST, which opens up new system-level architectures.

In the previous sections, multiple experimental prototypes and simulation studies of PECs enabled by the MV SiC technology have been presented for each application. Fig. 18 provides an overview across all applications in terms of their power, voltage, and switching frequency, where a filled circle indicates an experimentally validated prototype and a hollow one indicates a simulation study. The experimentally validated prototypes with ac or dc voltages of 8.5 kV or less shown in Fig. 18(a) have power ratings from tens of kVA up to 300 kVA and employ simple two- or three-level typologies. In the voltage range from 11 to 13.8 kV ac voltage, the four PECs targeted at grid applications have power ratings of 100 or 200 kVA and employ either two-level, three-level NPC, or five-level MMC typologies, where the two- and three-level typologies require series connection of the 10 or 15 kV SiC semiconductor devices. In comparison, most of the experimentally validated prototypes have switching frequencies ranging from 5 to 20 kHz with power ratings up to 300 kVA, as shown in Fig. 18(b). However, four PECs targeted at data center, electrolyzer, and charging of EV applications stand out as they have been experimentally demonstrated at 50 kHz for power ratings up to 25 kVA. The elevated switching frequencies are obtained by zero voltage switching of the SST-based typologies: SRC and DAB.

IV. Perspectives

The SiC technology has already penetrated multiple high-power electronic applications and incrementally started to

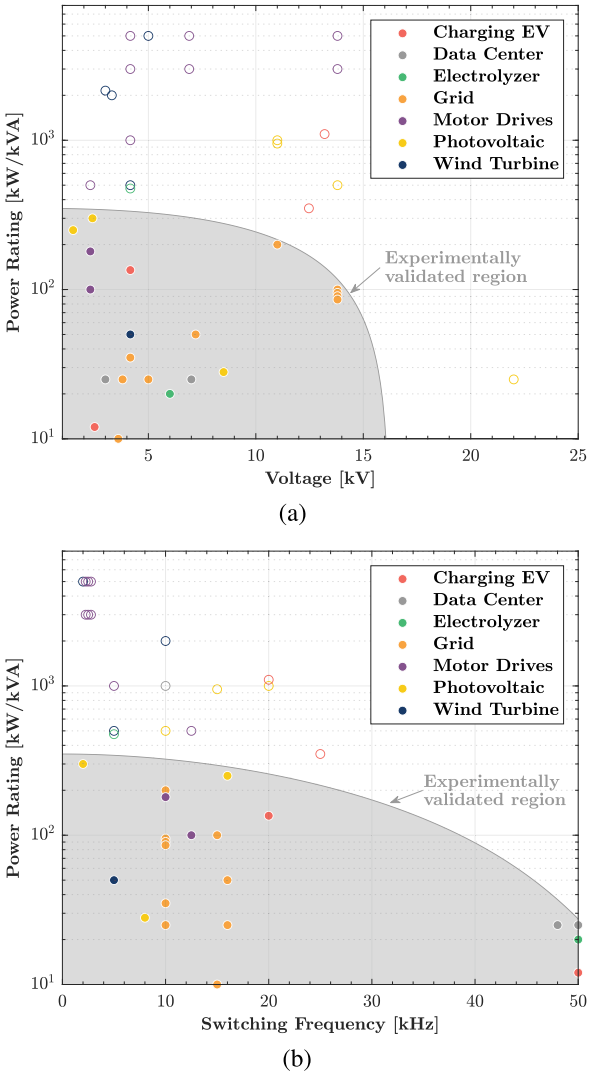

Fig. 18. Power rating of applications enabled by the MV SiC technology in terms of (a) voltage and (b) switching frequency. Filled indicates an experimentally validated prototype, while hollow indicates a simulation study. Data source: [212] to [310].

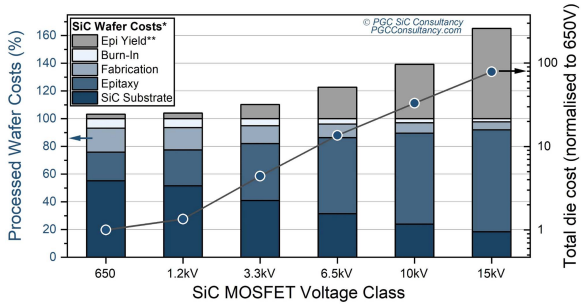

Fig. 19. PGC SiC Consultancy projected the cost of SiC MOSFET dies [314]. Copyright (2022) by PGC SiC Consultancy. *Reprinted with permission*.

replace the Si technology in applications where higher efficiency, higher blocking voltage capabilities, elevated switching frequencies, and/or better thermal performance are advantageous. As the SiC technology delivers promising technical advantages compared to its Si-counterparts, a further worldwide widespread is deemed unavoidable and their market share is expected to continuously grow in the coming years to support the electrification of society and the green transition.

The role of the MV SiC technology depends on several factors but foremost its maturity and thereof its availability and cost but also political incentives to support further technological advancements.

A. Availability

In the voltage range from 3.3 to 6.5 kV, multiple manufacturers have presented SiC MOSFET power modules with improved switching performance compared to the Si/SiC hybrid power modules as presented in Section II and expected to obtain parity in terms of power density within years of maturing. At and above 10 kV, the SiC MOSFETs and IGBTs open for new opportunities out of reach by the state-of-the-art Si technology, which indisputably puts the MV SiC technology in favor in this voltage range.

The first commercial widespread of MV SiC MOSFET power modules are expected to come from the 3.3 kV power modules in applications with dc-link voltages ranging from 1.5 to 2 kV. With the first 3.3 kV SiC MOSFET power modules becoming commercially available during 2024 from Wolfspeed and Mitsubishi, the commercial widespread has officially started. The authors strongly believe that other manufacturers will in the near future publish commercialized 3.3 kV SiC MOSFET power modules to enter the MV SiC market. In recent years, the semiconductor market has been driven by the automotive industry, which catalyzed the maturing process for 1.2 and 1.7 kV SiC MOSFETs to support their increasing demand; however, no such market driver is present for MV SiC MOSFETs and IGBTs, which inevitably prolongs their maturing process. With the potential market drivers benefiting from the MV SiC technology presented in Section III, the authors predict a strong potential for high-power electronic applications in the lower bound of MV, especially in the PV and automotive markets.

Although academia has shown increasing interest in MV SiC semiconductor devices and power modules with a wide voltage range from 3.3 to above 10 kV, research from academia is still limited due to excessive cost and restricted availability. With the increasing maturity of the MV SiC technology, the price reduction will allow broader research from academia to support the technological advancements.

B. Cost

The MV SiC technology needs to mature to a level at which the cost at the system-level becomes a cost-competitive solution compared to state-of-the-art technologies. Although further technological advancements within the MV SiC technology together with increased production volume inevitably push the price down, a price parity of the MV SiC technology with the MV Si- or LV SiC-counterparts is undoubtedly achieved within years. Projected prices from 2022 for both LV and MV SiC MOSFETs in terms of their breakdown voltage are given in Gammon et al.'s [314] work, presenting skyrocketing prices for SiC MOSFETs above 3.3 kV, as shown in Fig. 19. According to Casady and Palmour's [138] work, the absolute price for a single engineering

sample of 3.3 kV and 10 kV SiC MOSFET dies were in 2014 at a cost of \$5/kVA and \$6/kVA, respectively; however, prospected to drop down below \$1/kVA within years, under the assumption of a positive increase in production volume. Currently, as of 2024, the available prices on engineering samples of MV SiC MOSFET dies vary between \$2–\$5/kVA according to Power America [315], [316]. In comparison, commercially available MV Si/SiC hybrid and LV SiC MOSFET power modules, fully populated and encapsulated, have costs of less than \$ 1/kVA.

C. Policy-Making

Apart from the above-mentioned technical advantages presented by the MV SiC technology, the authors believe that policy-making is an essential tool to foster further technological advancements required to secure the commercial widespread. With the signing of the CHIPS and Science Act in the United States [317] and the European Chips Act in 2022 [318], the establishment of a political framework for strengthening the semiconductor ecosystem in both America and Europe was formally signed, which secured an equivalently three-digit billion-dollar public investment. Officially, the acts intend to bolster each region's competitiveness, catalyze regional economic growth and development, ensure the resilience of supply chains, and reduce external dependencies. Political initiatives such as the above-mentioned are crucial in securing a healthy economic ecosystem for semiconductor manufacturers to take the risk of expanding their manufacturing capabilities and pursue further technological advancements.

On this note, policy-making in terms of rules and regulations is not in place for emerging technologies enabled by the MV SiC technology, exemplified by EVs [267], [268], [269], [270] and microgrids [319], where standardization issues are discussed in detail for the implementation of SST-based typologies. To enable further technological development and commercial widespread, rules and regulations must be in place and should not be the bottleneck as it is now.

D. Technical Challenges

Several technical challenges remain, which need to be addressed by industry and academia to ensure robust and reliable operations of PECs enabled by the MV SiC technology.

1) Capacitive Couplings: Capacitive couplings have become a major concern in MV PECs in comparison to LV PECs, in which the power loop inductance has been a major concern [320]. Modeling, analysis, and optimization of parasitic capacitances are emerging topics currently being addressed by researchers [321], [322], [323], [324], [325], [326]. All components, including power modules, gate drivers, magnetic components, and voltage/current sensors, naturally contribute with parasitic capacitances, which under high dv/dt conditions cause large displacement current to circulate in the system.

2) Parasitic Inductance: Parasitic inductance in the power loop can cause overvoltage issues under high di/dt levels; however, the challenge is currently deemed less critical for MV PECs due to the reduced current levels as presented in Table II. Reduction of parasitic inductance remains a challenge for power module packaging and power stack designers [327], [328]. Eventually, the challenge will reappear for the 3.3 kV SiC MOSFET modules when the current scalability enables power modules to reach higher current levels.

3) Insulation and PD: Insulation and PD are two emerging topics for industry and academia that need to be comprehensively addressed. Due to the elevated voltage level in MV PECs, PD becomes by nature a more serious challenge as the electric fields are magnified. PD at triple points inside the power module [329], [330], [331], [332] and PD in all other system components experiencing square pulses with high dv/dt [333], [334], [335], [336], [337] poses challenges, which can lead to degradation and failure of insulation materials in power modules, magnetic components, gate drivers, etc.

4) Scalability of Power: Scalability of power in terms of either series or parallel connections of MV SiC semiconductor devices and power modules is unavoidable to reach the power capabilities required in high-power electronic applications. Major challenges pertaining to paralleling include passive and dynamic current sharing [338] and high-frequency gate oscillations during switching events [339], [340], [341], [342], which can result in nonuniform heat distribution among semiconductor devices and false turn-ON events. For series connection of MV SiC MOSFETs, the main challenge remains voltage balancing among the series connected devices [343] without sacrificing the performance by introducing additional snubber components and losses.

5) Gate Drivers: Gate drivers are key components to fully benefit from the MV SiC technology presented in Section II. Capacitive couplings, increased dv/dt, and PD in the gate driver and its auxiliary power supply are deemed the most critical challenges of now in relation to the MV SiC technology [93], [94], [205], [320]. The current trend is toward advanced gate driver designs of adaptive and active gate drivers capable of manipulating the switching behavior of the MV SiC semiconductor devices [344], [345], [346], [347] and optimized designs of the auxiliary power supplies [348], [349], [350], [351].

V. Conclusion

High-power PECs are indispensable in the electrification of society and the green transition. With the increasing power and efficiency requirements, the emerging MV SiC technology is a key enabler, which offers semiconductor devices and power modules with improved electrical performance compared to their Si-counterparts. Exhaustive lists of available MV SiC devices and power modules from both industry and academia are presented and give an overview of their recent advancements. A thorough review of typical high-power electronic applications has been presented and highlights the unique benefits of transitioning into the emerging MV SiC technology. At last, the future perspectives on the applicability and commercial widespread of the MV SiC technology have been presented. Apart from the remaining technical challenges, the restricted availability, excessive cost, and political engagement appear to be major challenges at present.

REFERENCES

[1] National Public Utilities Council, "Tracking U.S. electrification, by sector," Jul. 2023. Accessed: Feb. 2024. [Online]. Available: https://decarbonization.visualcapitalist.com/tracking-us-electrification-by-sector/

[2] International Energy Agency, "World energy outlook 2023," Oct. 2023. Accessed: Jan. 2024. [Online]. Available: https://www.iea.org/reports/world-energy-outlook-2023

[3] International Renewable Energy Agency, "World energy transitions outlook 2023: 1.5°C pathway, Volume 1," Jun. 2023. Accessed: Feb. 2024. [Online]. Available: https://mc-cd8320d4-36a1-40ac-83cc-3389-cdn-endpoint.azureedge.net/-/media/Files/IRENA/Agency/Publication/2023/Jun/IRENA_World_energy_transitions_outlook_2023.pdf?rev=db3ca01ecb4a4ef8accb31d017934e97

[4] Bloomberg, "New energy outlook 2022," 2023. Accessed: Dec. 2023. [Online]. Available: https://about.bnef.com/new-energy-outlook/

[5] DNV, "Energy transition outlook 2023," 2024. Accessed: Mar. 2024. [Online]. Available: https://www.dnv.com/energy-transition-outlook/

[6] McKinsey & Company, "Global energy perspective 2023," Oct. 2023. Accessed: Jan. 2024. [Online]. Available: https://www.mckinsey.com/industries/oil-and-gas/our-insights/global-energy-perspective-2023

[7] Tesla, "Supercharger," Accessed: Dec. 2023. [Online]. Available: https://www.tesla.com/supercharger

[8] ABB, "Terra HP Charger– Up to 350kW," Accessed: Dec. 2023. [Online]. Available: https://new.abb.com/ev-charging/high-power-charging

[9] Alpitronics, "Hypercharger by alpitronic," Accessed: Dec. 2023. [Online]. Available: https://www.hypercharger.it/

[10] Siemens, "SICHARGE D," Accessed: Dec. 2023. [Online]. Available: https://www.siemens.com/global/en/products/energy/emobility/sicharge-d.html

[11] Nidec, "DC Tower - 360kW," Accessed: Dec. 2023. [Online]. Available: https://www.nidec-industrial.com/products/ev-chargers/dc-tower-360/

[12] EVBox, "Troniq high power," Accessed: Dec. 2023. [Online]. Available: https://evbox.com/en/

[13] Kostad, "Unity epic charge 360kW," Accessed: Dec. 2023. [Online]. Available: https://www.kostad.at/en/unity-150-360-kw/

[14] SK Signet, "Powering your EV charging experience," Accessed: Dec. 2023. [Online]. Available: https://sksignet.us/distributed/400kw-dp--600kw-pc

[15] Tritium, "350kW high-powered charger," Accessed: Dec. 2023. [Online]. Available: https://tritiumcharging.com/product/pk-350/

[16] Charged EV, "ChargePoint's new 500kW DC fast charging platform," Nov. 2023. Accessed: Dec. 2023. [Online]. Available: https://chargedevs.com/newswire/chargepoints-new-500-kw-dc-fast-charging-platform-will-debut-as-the-power-behind-mercedess-new-us-charging-network/

[17] StarCharge, "Nova HPC system," Accessed: Dec. 2023. [Online]. Available: https://www.starcharge.com/details?id=MTI4NQ==

[18] S. Karimi, M. Zadeh, and J. A. Suul, "Shore charging for plug-in battery-powered ships: Power system architecture, infrastructure, and control," *IEEE Electrific. Mag.*, vol. 8, no. 3, pp. 47–61, Sep. 2020.

[19] Cavotec, "Electric vessels," Accessed: Dec. 2023. [Online]. Available: https://www.cavotec.com/en/your-applications/ports-maritime/automated-mooring/electric-vessels

[20] Wärtsilä, "Vessel battery charging," Accessed: Dec. 2023. [Online]. Available: https://www.wartsila.com/marine/products/ship-electrification-solutions/shore-power/charging

[21] DEIF, "Tycho Brahe - Hybrid ferry case story," 2019. Accessed: Dec. 2023. [Online]. Available: https://www.deif.com/media/subc3l04/tycho-brahe-uk-lowres.pdf

[22] Heliox, "Ultra-fast 600kW," Accessed: Dec. 2023. [Online]. Available: https://www.heliox-energy.com/products/ultra-fast-600kw-opportunity-charging

[23] Mobimar, "Nector 4000," 2019. Accessed: Dec. 2023. [Online]. Available: https://www.mobimar.com/application/files/2715/0460/5248/nector4000_brochure.pdf

[24] Riviera, "Color hybrid: Technology behind the world's largest plug-in hybrid ferry," Sep. 2019. Accessed: Dec. 2023. [Online]. Available: https://www.rivieramm.com/news-content-hub/news-content-hub/color-hybrid-technology-behind-the-worldrsquos-largest-plug-in-hybrid-ferry-56251

[25] European Alternative Fuels Observatory, "World's largest electric ferry launches in Norway (2021)," 2021. Accessed: Dec. 2023. [Online]. Available: https://alternative-fuels-observatory.ec.europa.eu/pilot-projects

[26] Zinus, "Shore power telescopic," Accessed: Dec. 2023. [Online]. Available: https://zinuspower.com/product/shore-power-telescopic/#functionality

[27] ABB, "Pantograph down for electric buses," Accessed: Dec. 2023. [Online]. Available: https://new.abb.com/ev-charging/pantograph-down

[28] Siemens, "SICHARGE UC family," Accessed: Dec. 2023. [Online]. Available: https://www.siemens.com/global/en/products/energy/emobility/sicharge-uc.html

[29] Stemmann-Technik, "FerryCHARGER - Charging solutions for electric ferries," Accessed: Dec. 2023. [Online]. Available: https://www.stemmann.com/en/products/charging_systems/ferrycharger

[30] APC by Schneider Electric, "Symmetra MW," Jan. 2012. Accessed: Feb. 2024. [Online]. Available: https://e-tecpowerman.com/wp-content/documents/Symmetra%20MW%20400kW%20to%201600kW.pdf

[31] Eaton, "PDI PowerHub 2 PDU," Jan. 2017. Accessed: Feb. 2024. [Online]. Available: https://www.eaton.com/us/en-us/catalog/backup-power-ups-surge-it-power-distribution/eaton-pdi-powerhub-2-pdu.html

[32] Toshiba, "G9000 series 2000kVA," Oct. 2017. Accessed: Feb. 2024. [Online]. Available: https://www.toshiba.com/tic/power-electronics/uninterruptible-power-systems/three-phase/g9000-series-100-to-2000-kva

[33] ABB, "PCS120 MV UPS," Jan. 2018. Accessed: Feb. 2024. [Online]. Available: https://image.indotrading.com/co93602/pdf/p753761/abb%20pcs120%20mv%20ups.pdf

[34] ABB, "Cyberex PDU 1.3MW," Jan. 2019. Accessed: Feb. 2024. [Online]. Available: https://new.abb.com/ups/power-distribution/power-distribution-unit/power-distribution-unit

[35] Mitsubishi Electric, "9900D data sheet," Sep. 2019. Accessed: Feb. 2024. [Online]. Available: https://www.jantechups.com/wp-content/uploads/2020/01/sa-enl-0061-9900d-data-sheet.pdf

[36] Borri, "UPSaver 3vo," Feb. 2020. Accessed: Feb. 2024. [Online]. Available: https://www.borri.it/product/upsaver-modular-ups/

[37] Kstar, "Modular UPS," Apr. 2020. Accessed: Feb. 2024. [Online]. Available: https://www.kstar.com/ModularUPS/15690.jhtml

[38] Kohler, "MF Series," Sep. 2020. Accessed: Feb. 2024. [Online]. Available: https://www.kohler-ups.co.uk/product/kohler-mf-series/

[39] ABB, "HiPerGuard," Jan. 2020. Accessed: Feb. 2024. [Online]. Available: https://search.abb.com/library/Download.aspx?DocumentID=2UCD301143-P&LanguageCode=en&DocumentPartId=&Action=Launch

[40] Legrand, "Keor XPE — Scalable high-power UPS," Feb. 2021. Accessed: Feb. 2024. [Online]. Available: https://ups.legrand.com/media/document/brochure-keor-xpe-gb.pdf

[41] Huawei, "Fusion power 6000," Jan. 2021. Accessed: Feb. 2024. [Online]. Available: https://digitalpower.huawei.com/en/data-center-facility/product_solution/dce_intelligent_power_supply/detail/118.html

[42] Vertiv, "Liebert trinergy cube," Aug. 2022. Accessed: Feb. 2024. [Online]. Available: https://www.vertiv.com/49c465/globalassets/products/critical-power/uninterruptible-power-supplies-ups/trinergy-cube-150-kw-3.4-mw-interactive-brochure-english.pdf

[43] Piller, "Piller installs 3.6 MW UPS systems with li-ion energy storage at German data centre," Aug. 2023. Accessed: Feb. 2024. [Online]. Available: https://www.piller.com/article/piller-installs-3-6-mw-ups-systems-with-li-ion-energy-storage-at-german-data-centre/

[44] Nel Hydrogen, "Atmospheric alkaline electrolyser," Accessed: Dec. 2023. [Online]. Available: https://nelhydrogen.com/product/atmospheric-alkaline-electrolyser-a-series/

[45] JohnCockerill, "DQ1000 alkaline electrolyser," Nov. 2023. Accessed: Dec. 2023. [Online]. Available: https://hydrogen.johncockerill.com/wp-content/uploads/sites/3/2023/04/dq-1000-def-2-hd-en.pdf

[46] Cummins– Hydrogenics, "MW-scale PEM electrolysis," Sep. 2020. Accessed: Dec. 2023. [Online]. Available: https://hybalance.eu/wp-content/uploads/2020/09/20200924_HyBalance_Hydrogenics_vFINAL.pdf

[47] Elogen, "PEM-Electrolysers," Dec. 2023. Accessed: Dec. 2023. [Online]. Available: https://elogenh2.com/wp-content/uploads/2023/11/Product-Overview-Elogen-November-2023.pdf

[48] Plug Power, "EX-2125D electrolyzer," Apr. 2022. Accessed: Dec. 2023. [Online]. Available: https://www.plugpower.com/hydrogen/electrolyzer-hydrogen/

[49] H-TEC Systems, "PEM electrolyzer," Aug. 2023. Accessed: Dec. 2023. [Online]. Available: https://www.h-tec.com/fileadmin/user_upload/produkte/produktseiten/MHP/spec-sheet/H-TEC-Datenblatt-MHP-EN-23-08.pdf

[50] Asahi Kasei, "Asahi Kasei starts construction of alkaline water electrolysis pilot test plant for hydrogen production," Nov. 2022. Accessed: Dec. 2023. [Online]. Available: https://www.asahi-kasei.com/news/2022/e221107.html

[51] Green Hydrogen Systems, "HyProvide X-series," Accessed: Dec. 2023. [Online]. Available: https://www.greenhydrogensystems.com/electrolysers/hyprovide-x-series-6mw-modular-electrolyser

[52] Stargate Hydrogen, "Gateway series," Feb. 2023. Accessed: Dec. 2023. [Online]. Available: https://stargatehydrogen.com/wp-content/uploads/2023/02/Stargate-Brochure-Feb-2023.pdf

[53] Sunfire, "Hydrogen, The renewable feedstock and energy carrier," Accessed: Dec. 2023. [Online]. Available: https://www.sunfire.de/en/hydrogen

[54] Thyssenkrupp Nucera, "Green hydrogen solutions," Accessed: Dec. 2023. [Online]. Available: https://thyssenkrupp-nucera.com/green-hydrogen-solutions/

[55] ITM Power, "Leading PEM electrolyser technology," Accessed: Dec. 2023. [Online]. Available: https://itm-power.com/products/

[56] McPhy, "McLyzer product line," Jun. 2023. Accessed: Dec. 2023. [Online]. Available: https://cellar-c2.services.clever-cloud.com/com-mcphy/uploads/2023/06/2023_McLyzer-Product-Line-EN.pdf

[57] Siemens Energy, "Green hydrogen production," Accessed: Dec. 2023. [Online]. Available: https://assets.siemens-energy.com/siemens/assets/api/uuid:2a5fca2e-994e-45f3-859a-6fd4b0fc831c/m9-green-hydrogen-production.pdf

[58] GE Power Conversion, "Power electronics MV7000," 2019. Accessed: Jan. 2024. [Online]. Available: https://www.gepowerconversion.com/product-solutions/medium-voltage-drives/mv7000

[59] Innomotics- A Siemens Business, "SINAMICS medium voltage drives," Accessed: Jan. 2024. [Online]. Available: https://www.innomotics.com/en/products/converters/medium-voltage-converters.html

[60] ABB, "ABB medium voltage AC drives," Accessed: Jan. 2024. [Online]. Available: https://new.abb.com/drives/medium-voltage-ac-drives

[61] SMA, "Sunny central 630HE," Jan. 2010. Accessed: Jan. 2024. [Online]. Available: https://files.sma.de/downloads/SC500_630HE-DUS103515W.pdf

[62] ABB, "Central inverters PVS800," Jan. 2011. Accessed: Jan. 2024. [Online]. Available: https://new.abb.com/docs/librariesprovider22/technical-documentation/pvs800-central-inverters-flyer.pdf?sfvrsn=2

[63] Ingeteam, "Ingeteam launches a 1500 Vdc central inverter for large PV plants," Jun. 2016. Accessed: Jan. 2024. [Online]. Available: https://www.ingeteam.com/cz/Pressroom/tabid/3382/articleType/ArticleView/articleId/1114/language/cs-CZ/Ingeteam-launches-a-1500-Vdc-central-inverter-for-large-PV-plants.aspx

[64] ABB, "Central inverters PVS800," Sep. 2019. Accessed: Jan. 2024. [Online]. Available: https://www.fimer.com/sites/default/files/PVS800_central_inverters_flyer_3AUA0000057380_RevN_EN_lowres.pdf

[65] TMEIC, "Solar ware 3200," Jul. 2017. Accessed: Jan. 2024. [Online]. Available: https://www.tmeic.com/products/solar-ware-3200

[66] Sungrow, "There's more to it than just turning DC to AC," Accessed: Jan. 2024. [Online]. Available: https://en.sungrowpower.com/ProductsHome/14/15/turnkey-solution

[67] ABB, "Central inverters PVS980," Nov. 2019. Accessed: Jan. 2024. [Online]. Available: https://new.abb.com/news/detail/23761/abb-launches-next-generation-central-inverter-with-unique-cooling-capabilities

[68] SMA, "Sunny central 2475," Jan. 2020. Accessed: Jan. 2024. [Online]. Available: https://www.sma.de/en/products/solarinverters/sunny-central-2200-2475

[69] Siemens, "SINACON PV," Jan. 2020. Accessed: Jan. 2024. [Online]. Available: https://assets.new.siemens.com/siemens/assets/api/uuid:cb65b0d3-6425-48f5-92cb-cc217d2d5285/sinacon-pv-technical-data-en.pdf

[70] Power Electronics, "HEMK," Accessed: Jan. 2024. [Online]. Available: https://power-electronics.com/en/solar/hemk

[71] SMA, "Sunny central 4600 UP," Jan. 2022. Accessed: Jan. 2024. [Online]. Available: https://files.sma.de/downloads/SC4xxxUP-DS-en-30.pdf

[72] Gamesa Electric, "Proteus PCS Inverters," Jan. 2022. Accessed: Jan. 2024. [Online]. Available: https://assets.new.siemens.com/siemens/assets/api/uuid:13122164-bffe-4729-bece-3ac8f96ed9e6/ELE-Proteus-PCS-Inverters-AC-Storage-DAT.pdf

[73] Ingeteam, "Ingecon Sun MSK," Accessed: Jan. 2024. [Online]. Available: https://www.ingeteam.com/de/de-de/energie/photovoltaik/p15_24_575_0/ingecon-sun-msk.aspx

[74] Alencon, "GrIP: Alencon's 10 MW PV central inverter," Accessed: Jan. 2024. [Online]. Available: https://alenconsystems.com/central-inverters-1/

[75] Siemens, "Photovoltaic systems for utility-scale solar power plants," Accessed: Jan. 2024. [Online]. Available: https://www.siemens.com/global/en/products/energy/medium-voltage/solutions/electrical-balance.html

[76] Enercon, "Global manufacturer of wind turbines," Accessed: Jan. 2024. [Online]. Available: https://www.enercon.de/en

[77] Vestas, "Wind turbine product portfolio," Accessed: Jan. 2024. [Online]. Available: https://us.vestas.com/en-us/products

[78] Dongfang Electric Corporation, "Large capacity direct drive wind turbine," Dec. 2023. Accessed: Jan. 2024. [Online]. Available: https://www.beltandroadassociates.com/wp-content/uploads/2020/12/DEC-Wind-Power-Brochure-S.pdf

[79] OffshoreWind, "China's first 8 MW wind turbine stands offshore," Apr. 2020. Accessed: Jan. 2024. [Online]. Available: https://www.offshorewind.biz/2020/04/28/chinas-first-8-mw-wind-turbine-stands-offshore/

[80] OffshoreWind, "First MySE8.3-180 wind turbine stands offshore," Jan. 2021. Accessed: Jan. 2024. [Online]. Available: https://www.offshorewind.biz/2021/01/19/first-myse8-3-180-wind-turbine-stands-offshore/

[81] OffshoreWind, "DEC rolls out 13 MW offshore wind turbine," Feb. 2022. Accessed: Jan. 2024. [Online]. Available: https://www.offshorewind.biz/2022/02/23/dec-rolls-out-13-mw-offshore-wind-turbine/

[82] MingYang Smart Energy, "MySE11-203, Hybrid drives the world," 2022. Accessed: Jan. 2024. [Online]. Available: https://www.myse.com.cn/en/wind-turbine/index.aspx

[83] Siemens Gamesa Renewable Energy, "Scaling up the use of offshore wind turbines," Accessed: Jan. 2024. [Online]. Available: https://www.siemensgamesa.com/en-int/products-and-services/offshore

[84] GE Renewable Energy, "Haliade-X offshore wind turbine," Accessed: Jan. 2024. [Online]. Available: https://www.ge.com/renewableenergy/wind-energy/offshore-wind/haliade-x-offshore-turbine

[85] Electrek, "The world's largest wind turbine is now installed in China," Jun. 2023. Accessed: Jan. 2024. [Online]. Available: https://electrek.co/2023/06/29/the-worlds-largest-wind-turbine-is-now-being-installed-in-china/

[86] OffshoreWind, "Goldwind launches 12 MW offshore wind turbine, targets Chinese market for now," Nov. 2023. Accessed: Jan. 2024. [Online]. Available: https://www.offshorewind.biz/2021/11/02/goldwind-launches-12-mw-offshore-wind-turbine-targets-chinese-market-for-now/

[87] Sciencealert, "The largest and most powerful wind turbine ever built is now operational," Jul. 2023. Accessed: Jan. 2024. [Online]. Available: https://www.sciencealert.com/the-largest-and-most-powerful-wind-turbine-ever-built-is-now-operational

[88] OffshoreWind, "GE developing 18 MW Haliade-x offshore wind turbine," Mar. 2023. Accessed: Jan. 2024. [Online]. Available: https://www.offshorewind.biz/2023/03/14/ge-developing-18-mw-haliade-x-offshore-wind-turbine/

[89] CSSC Haizhung, "CSSC Haizhuang H260-18MW offshore wind turbine giant emerges," Jan. 2023. Accessed: Jan. 2024. [Online]. Available: https://cssc-hz.com/?en/enNews/NewsReleases/148.html

[90] OffshoreWind, "22 MW offshore wind turbine in the works for 2024/25," Oct. 2023. Accessed: Jan. 2024. [Online]. Available: https://www.offshorewind.biz/2023/10/23/22-mw-offshore-wind-turbine-in-the-works-for-2024-25/

[91] International Electrotechnical Commission, "Understanding standards," Accessed: Jan. 2024. [Online]. Available: https://www.iec.ch/understanding-standards

[92] American National Standards Institute, "We facilitate standardization solutions," Jan. 2024. Accessed: Jan. 2024. [Online]. Available: https://www.ansi.org/

[93] S. Ji, Z. Zhang, and F. Wang, "Overview of high voltage SiC power semiconductor devices: Development and application," *CES Trans. Elect. Mach. Syst.*, vol. 1, no. 3, pp. 254–264, Sep. 2017.

[94] B. Hu et al., "A survey on recent advances of medium voltage silicon carbide power devices," in *2018 IEEE Energy Convers. Congr. Expo.*, 2018, pp. 2420–2427.

[95] F. Wang and S. Ji, "Benefits of high-voltage SiC-based power electronics in medium-voltage power-distribution grids," *Chin. J. Elect. Eng.*, vol. 7, no. 1, pp. 1–26, Mar. 2021.

[96] M. Adler, K. Owyang, B. Baliga, and R. Kokosa, "The evolution of power device technology," *IEEE Trans. Electron Devices*, vol. 31, no. 11, pp. 1570–1591, Nov. 1984.

[97] P. Steimer, H. E. Gruning, J. Werninger, E. Carroll, S. Klaka, and S. Linder, "IGCT—A new emerging technology for high power, low cost inverters," *IEEE Ind. Appl. Mag.*, vol. 5, no. 4, pp. 12–18, Jul./Aug. 1999.

[98] Y. Suh and P. K. Steimer, "Application of IGCT in high-power rectifiers," *IEEE Trans. Ind. Appl.*, vol. 45, no. 5, pp. 1628–1636, Sep./Oct. 2009.

[99] N. Iwamuro and T. Laska, "IGBT history, state-of-the-art, and future prospects," *IEEE Trans. Electron Devices*, vol. 64, no. 3, pp. 741–752, Mar. 2017.

[100] T. Fujii et al., "4.5 kV-2000 A power pack IGBT (ultra high power flat-packaged PT type RC-IGBT)," in *Proc. 12th Int. Symp. Power Semicond. Devices ICs Proc.*, 2000, pp. 33–36.

[101] B. Baliga, "The future of power semiconductor device technology," *Proc. IEEE Proc. IRE*, vol. 89, no. 6, pp. 822–832, Jun. 2001.

[102] J. Millán, P. Godignon, X. Perpiñà, A. Pérez-Tomás, and J. Rebollo, "A survey of wide bandgap power semiconductor devices," *IEEE Trans. Power Electron.*, vol. 29, no. 5, pp. 2155–2163, May 2014.

[103] X. She, A. Q. Huang, O. Lucía, and B. Ozpineci, "Review of silicon carbide power devices and their applications," *IEEE Trans. Ind. Electron.*, vol. 64, no. 10, pp. 8193–8205, Oct. 2017.

[104] A. Nabae, I. Takahashi, and H. Akagi, "A new neutral-point-clamped PWM inverter," *IEEE Trans. Ind. Appl.*, vol. IA-17, no. 5, pp. 518–523, Sep. 1981.

[105] H. Akagi, "Multilevel converters: Fundamental circuits and systems," *Proc. IEEE Proc. IRE,* vol. 105, no. 11, pp. 2048–2065, Nov. 2017.

[106] A. Dekka, B. Wu, R. L. Fuentes, M. Perez, and N. R. Zargari, "Evolution of topologies, modeling, control schemes, and applications of modular multilevel converters," *IEEE Trans. Emerg. Sel. Topics Power Electron.*, vol. 5, no. 4, pp. 1631–1656, Dec. 2017.

[107] R. Marquardt, "Modular multilevel converters: State of the art and future progress," *IEEE Power Electron. Mag.*, vol. 5, no. 4, pp. 24–31, Dec. 2018.

[108] L. Han, L. Liang, Y. Kang, and Y. Qiu, "A review of SiC IGBT: Models, fabrications, characteristics, and applications," *IEEE Trans. Power Electron.*, vol. 36, no. 2, pp. 2080–2093, Feb. 2021.

[109] F. Wang and H. Li, "Survey and benchmark of benefits of high voltage SiC applications in medium voltage power distribution grids," Oak Ridge Nat. Lab., Oak Ridge, TN, USA, Tech. Rep. ORNL/TM-2022/2561, Nov. 2022. Accessed: Feb. 2024. [Online]. Available: https://www.osti.gov/biblio/1922316

[110] T. P. Chow, "Wide bandgap semiconductor power devices for energy efficient systems," in *2015 IEEE 3rd Workshop Wide Bandgap Power Devices Appl.*, 2015, pp. 402–405.

[111] M. Östling, R. Ghandi, and C.-M. Zetterling, "SiC power devices — Present status, applications and future perspective," in *2011 IEEE 23rd Int. Symp. Power Semicond. Devices ICs*, 2011, pp. 10–15.

[112] T. Kimoto and Y. Yonezawa, "Current status and perspectives of ultrahigh-voltage SiC power devices," *Mater. Sci. Semicond. Process.*, vol. 78, pp. 43–56, 2018. [Online]. Available: https://www.sciencedirect.com/science/article/pii/S1369800117319066

[113] L. Sang et al., "Development of high-voltage SiC power electronic devices," in *2021 18th China Int. Forum Solid State Lighting 2021 7th Int. Forum Wide Bandgap Semicond.*, 2021, pp. 17–24.

[114] B. J. Baliga, "Silicon carbide power devices: Progress and future outlook," *IEEE Trans. Emerg. Sel. Topics Power Electron.*, vol. 11, no. 3, pp. 2400–2411, Jun. 2023.

[115] D. Johannesson, M. Nawaz, K. Jacobs, S. Norrga, and H.-P. Nee, "Potential of ultra-high voltage silicon carbide semiconductor devices," in *2016 IEEE 4th Workshop Wide Bandgap Power Devices Appl.*, 2016, pp. 253–258.

[116] R. J. Callanan et al., "Recent progress in SiC DMOSFETs and JBS diodes at Cree," in *2008 34th Annu. Conf. IEEE Ind. Electron.*, 2008, pp. 2885–2890.

[117] J. B. Casady et al., "New generation 10kV SiC power MOSFET and diodes for industrial applications," in *Proc. PCIM Europe 2015; Int. Exhib. Conf. Power Electron., Intell. Motion, Renewable Energy Energy Manage.*, 2015, pp. 1–8.

[118] J. W. Palmour et al., "Silicon carbide power MOSFETs: Breakthrough performance from 900 V up to 15kV," in *2014 IEEE 26th Int. Symp. Power Semicond. Devices IC's*, 2014, pp. 79–82.

[119] J. W. Palmour, "Silicon carbide power device development for industrial markets," in *2014 IEEE Int. Electron Devices Meeting*, 2014, pp. 1.1.1–1.1.8.

[120] V. Pala et al., "10kV and 15kV silicon carbide power MOSFETs for next-generation energy conversion and transmission systems," in *2014 IEEE Energy Convers. Congr. Expo.*, 2014, pp. 449–454.

[121] D. Grider et al., "10kV/120 A SiC DMOSFET half H-bridge power modules for 1 MVA solid state power substation," in *2011 IEEE Electric Ship Technol. Symp.*, 2011, pp. 131–134.

[122] A. Kadavelugu et al., "Characterization of 15kV SiC n-IGBT and its application considerations for high power converters," in *2013 IEEE Energy Convers. Congr. Expo.*, 2013, pp. 2528–2535.

[123] K. Fukuda et al., "Development of ultrahigh-voltage SiC devices," *IEEE Trans. Electron Devices*, vol. 62, no. 2, pp. 396–404, Feb. 2015.

[124] E. Van Brunt, D. Grider, V. Pala, S.-H. Ryu, J. Casady, and J. Palmour, "Development of medium voltage SiC power technology for next generation power electronics," in *2015 IEEE Int. Workshop Integr. Power Packag.*, 2015, pp. 72–74.

[125] M. Sakai et al., "3.3kV SiC power module with low switching loss," *SEI Tech. Rev.*, vol. 81, pp. 51–55, 2015.

[126] T. Sakaguchi, M. Aketa, T. Nakamura, M. Nakanishi, and M. Rahimo, "Characterization of 3.3kV and 6.5kV SiC MOSFETs," in *Proc. PCIM Europe 2017; Int. Exhib. Conf. Power Electron., Intell. Motion, Renewable Energy Energy Manage.*, 2017, pp. 1–5.

[127] R. Minamisawa and A. Mihaila, "AMPERE advanced materials for power electronics devices," 2021. Accessed: Mar. 2024. [Online]. Available: https://www.aramis.admin.ch/Default?DocumentID=68491&Load=true

[128] V. Pala, E. Van Brunt, B. Hull, S. Allen, and J. W. Palmour, "Silicon carbide MOSFETs for medium voltage megawatt scale systems," in *Silicon Carbide and Related Materials 2015* (Materials Science Forum Series), vol. 858. Wollerau, Switzerland: Trans Tech Pub. Ltd., 2016, pp. 970–973.

[129] E. Van Brunt et al., "Reliability assessment of a large population of 3.3kV, 45 A 4H-SIC MOSFETs," in *2017 29th Int. Symp. Power Semicond. Devices IC's*, 2017, pp. 251–254.

[130] V. Mulpuri, S. Jadav, S. Sundaresan, and R. Singh, "Characterization and robustness evaluation of 3.3kV/40 mΩ SiC DMOSFETs," in *2019 IEEE 7th Workshop Wide Bandgap Power Devices Appl.*, 2019, pp. 130–136.

[131] J. L. Hostetler et al., "6.5kV enhancement mode SiC JFET based power module," in *2015 IEEE 3rd Workshop Wide Bandgap Power Devices Appl.*, 2015, pp. 300–305.

[132] S. Sabri et al., "New generation 6.5kV SiC power MOSFET," in *2017 IEEE 5th Workshop Wide Bandgap Power Devices Appl.*, 2017, pp. 246–250.

[133] S. Wirths et al., "High-k dielectrics for SiC power MOSFET technology: Unrivaled reliability, ruggedness and performance," 2021. Accessed: Mar. 2024. [Online]. Available: https://library.e.abb.com/public/1c9a9e10fc7f493196d56b2c55daa993/Hitachi_Energy_High-k-dielectrics-for-SiC-power-MOSFET-technology.pdf?x-sign=5NHR8ahVQZb/uphZU3kgXjQHAUSfbgWUdRwEF2m5dgQj1IcA4vuh+7VrTuF3Eu87

[134] S.-H. Ryu, S. Krishnaswami, B. Hull, J. Richmond, A. Agarwal, and A. Hefner, "10kV, 5A 4H-SiC power DMOSFET," in *2006 IEEE Int. Symp. Power Semicond. Devices IC's*, 2006, pp. 1–4.

[135] J. Wang et al., "Characterization, modeling, and application of 10-kV SiC MOSFET," *IEEE Trans. Electron Devices*, vol. 55, no. 8, pp. 1798–1806, Aug. 2008.

[136] Q. C. J. Zhang et al., "10 kV, 10A bipolar junction transistors and Darlington transistors on 4H-SiC," in *Silicon Carbide and Related Materials 2009* (Materials Science Forum Series), vol. 645. Wollerau, Switzerland: Trans Tech Pub. Ltd, 2010, pp. 1025–1028.

[137] S. Sundaresan, S. Jeliazkov, B. Grummel, and R. Singh, "10kV SiC BJTs — Static, switching and reliability characteristics," in *2013 25th Int. Symp. Power Semicond. Devices IC's*, 2013, pp. 303–306.

[138] J. Casady and J. Palmour, "Power products commercial roadmap for SiC from 2012-2020 and pricing forecasts for 650N-15kV SiC power module," 2014. Accessed: Mar. 2024. [Online]. Available: https://www.nist.gov/document/approved-cassadypalmourpptx

[139] M. K. Das et al., "A 13kV 4H-SiC n-channel IGBT with low Rdiff, on and fast switching," in *Silicon Carbide and Related Materials 2007* (Materials Science Forum Series), vol. 600. Wollerau, Switzerland: Trans Tech Pub. Ltd, 2009, pp. 1183–1186.

[140] S.-H. Ryu et al., "High performance, ultra high voltage 4H-SiC IGBTs," in *2012 IEEE Energy Convers. Congr. Expo.*, 2012, pp. 3603–3608.

[141] D. Grider et al., "Advanced SiC power technology for high megawatt power conditioning," May 2012. Accessed: Feb. 2024. [Online]. Available: https://www.nist.gov/system/files/documents/pml/high_megawatt/Grider-Cree.pdf

[142] L. Cheng et al., "Development of low $R_{on,diff}$, 12kV, 4H-SiC GTOs for high-power and high-temperature applications," in *Proc. Additional Conf. (Device Packag., HiTEC, HiTEN, CICMT)*, vol. 2012, 2012, pp. 000149–000153, doi: 10.4071/HITEC-2012-WA13.

[143] Y. Yonezawa et al., "Low Vf and highly reliable 16kV ultrahigh voltage SiC flip-type n-channel implantation and epitaxial IGBT," in *2013 IEEE Int. Electron Devices Meeting*, 2013, pp. 6.6.1–6.6.4.

[144] T. Mizushima et al., "Dynamic characteristics of large current capacity module using 16-kV ultrahigh voltage SiC flip-type n-channel IE-IGBT," in *2014 IEEE 26th Int. Symp. Power Semicond. Devices IC's*, 2014, pp. 277–280.

[145] X. Yang, Y. Tao, T. Yang, R. Huang, and B. Song, "Fabrication of 4H-SiC n-channel IGBTs with ultra high blocking voltage," *J. Semicond.*, vol. 39, no. 3, Mar. 2018, Art. no. 034005, doi: 10.1088/1674-4926/39/3/034005.

[146] S. H. Ryu et al., "15 Kv n-GTOs in 4H-SiC," in *Silicon Carbide and Related Materials 2018* (Materials Science Forum Series), vol. 963. Wollerau, Switzerland: Trans Tech Pub. Ltd, 2019, pp. 651–654.

[147] X. Wang and J. A. Cooper, "High-voltage n-channel IGBTs on free-standing 4H-SiC epilayers," *IEEE Trans. Electron Devices*, vol. 57, no. 2, pp. 511–515, Feb. 2010.

[148] S. Ryu et al., "Ultra high voltage IGBTs in 4H-SiC," in *Proc. 1st IEEE Workshop Wide Bandgap Power Devices Appl.*, 2013, pp. 36–39.

[149] E. V. Brunt et al., "22kV, 1 cm^2, 4H-SiC n-IGBTs with improved conductivity modulation," in *2014 IEEE 26th Int. Symp. Power Semicond. Devices IC's*, 2014, pp. 358–361.

[150] S. H. Ryu et al., "20kV 4H-SiC N-IGBTs," in *Silicon Carbide and Related Materials 2013* (Materials Science Forum Series), vol. 778. Wollerau, Switzerland: Trans Tech Pub. Ltd., 2014, pp. 1030–1033.

[151] L. Cheng et al., "20kV, 2 cm^2, 4H-SIC gate turn-off thyristors for advanced pulsed power applications," in *Proc. IEEE 2013 Pulsed Power Conf.*, 2013, pp. 1–4.

[152] E. van Brunt et al., "27 Kv, 20A. 4H-SiC n-IGBTs," in *Silicon Carbide and Related Materials 2014* (Materials Science Forum Series), vol. 821. Wollerau, Switzerland: Trans Tech Pub. Ltd., 2015, pp. 847–850.

[153] Dynex, "Dynex IGBT modules," Accessed: Mar. 2024. [Online]. Available: https://www.dynexsemi.com/IGBT

[154] Infineon, "IGBT modules," Accessed: Mar. 2024. [Online]. Available: https://www.infineon.com/cms/en/product/power/igbt/igbt-modules/

[155] Minebea, "High voltage IGBT/SiC," Accessed: Jun. 2024. [Online]. Available: https://www.minebea-psd.com/en/products/igbt/index.html

[156] Y. Li et al., "State-of-the-art medium- and high-voltage silicon carbide power modules, challenges and mitigation techniques: A review," *IEEE Trans. Compon. Packag. Manuf. Technol.*, to be published, doi: 10.1109/TCPMT.2024.3391653.

[157] J. B. Casady, T. McNutt, D. Girder, and J. Palmour, "Medium voltage SiC R&D update," in *Wolfspeed*, vol. 16, pp. 4317–4327, 2016.

[158] K. Hamada et al., "3.3kV/1500 A power modules for the world's first all-SiC traction inverter," *Japanese J. Appl. Phys.*, vol. 54, no. 4S, Feb. 2015, Art. no. 04DP07.

[159] J. Hayes et al., "Dynamic characterization of next generation medium voltage (3.3kV, 10kV) silicon carbide power modules," in *Proc. PCIM Europe 2017; Int. Exhib. Conf. Power Electron., Intell. Motion, Renewable Energy Energy Manage.*, 2017, pp. 1–7.

[160] R. Takayanagi et al., "3.3kV All-SiC module for electric distribution equipment," in *2018 Int. Power Electron. Conf.*, 2018, pp. 3396–3400.

[161] B. Mouawad, A. Hussein, and A. Castellazzi, "A 3.3kV SiC MOSFET half-bridge power module," in *Proc. CIPS 2018 10th Int. Conf. Integr. Power Electron. Syst.*. VDE, 2018, pp. 1–6.

[162] K. Yasui et al., "A 3.3kV 1000 A high power density SiC power module with sintered copper die attach technology," in *Proc. PCIM Europe 2019; Int. Exhib. Conf. Power Electron., Intell. Motion, Renewable Energy Energy Manage*. VDE, 2019, pp. 1–6.

[163] S. Kicin et al., "Ultra-fast switching 3.3kV SiC high-power module," in *Proc. PCIM Europe Digit. Days 2020; Int. Exhib. Conf. Power Electron., Intell. Motion, Renewable Energy Energy Manage.* VDE, 2020, pp. 1–8.

[164] H. Kono et al., "3.3kV all SiC MOSFET module with Schottky barrier diode embedded SiC MOSFET," in *Proc. PCIM Europe Digit. Days 2021; Int. Exhib. Conf. Power Electron., Intell. Motion, Renewable Energy Energy Manage.*, 2021, pp. 1–6.

[165] Z. Guo, L. Zhang, S. Sen, and A. Q. Huang, "A novel 3.6kV/400A SiC intelligent power module (IPM)," in *2021 IEEE Appl. Power Electron. Conf. Expo.*, 2021, pp. 39–43.

[166] Y. Sekino et al., "3.3kV all SiC module with 2nd generation trench gate SiC MOSFETs for traction," in *Proc. PCIM Europe 2022; Int. Exhib. Conf. Power Electron., Intell. Motion, Renewable Energy Energy Manage.* VDE, 2022, pp. 1–7.

[167] Y. Li et al., "Design, fabrication and testing of 3.3kV/200A SiC half-bridge power module," in *2023 IEEE Appl. Power Electron. Conf. Expo.*, 2023, pp. 331–335.

[168] Y. Chen et al., "3.3kV low-inductance full SiC power module," in *2023 IEEE Appl. Power Electron. Conf. Expo.*, 2023, pp. 2634–2640.

[169] A. H. Ismail, A. Al-Hmoud, Y. Zhao, A. Kumar, and K. Olejniczak, "Characterization and system benefits of using 3.3kV all-SiC MOSFET modules in MV power converter applications," in *Proc. PCIM Europe 2023; Int. Exhib. Conf. Power Electron., Intell. Motion, Renewable Energy Energy Manage.*, 2023, pp. 1–7.

[170] J.-I. Nakashima et al., "6.5-kV full-SiC power module (HV100) with SBD-embedded SiC-MOSFETs," in *Proc. PCIM Europe 2018; Int. Exhib. Conf. Power Electron., Intell. Motion, Renewable Energy Energy Manage*. VDE, 2018, pp. 1–7.

[171] B. DeBoi, A. Lemmon, B. Nelson, C. New, and D. Hudson, "Modeling and validation of medium voltage SiC power modules," in *2020 IEEE Appl. Power Electron. Conf. Expo.*, 2020, pp. 1964–1971.

[172] L. Zhang, S. Sen, and A. Q. Huang, "7.2-kV/60-A austin SuperMOS: An intelligent medium-voltage SiC power switch," *IEEE Trans. Emerg. Sel. Topics Power Electron.*, vol. 8, no. 1, pp. 6–15, Mar. 2020.

[173] D. Yujie et al., "Fabrication and dynamic switching characteristics of 6.5kV 400A SiC MOSFET module," in *2020 17th China Int. Forum Solid State Lighting 2020 Int. Forum Wide Bandgap Semicond. China*, 2020, pp. 67–70.

[174] L. Ma et al., "A double-sided cooling 6.5kV SiC MOSFET power module with insulation enhancement design," in *2023 IEEE Appl. Power Electron. Conf. Expo.*, 2023, pp. 2550–2555.

[175] B. Passmore et al., "The next generation of high voltage (10kV) silicon carbide power modules," in *2016 IEEE 4th Workshop Wide Bandgap Power Devices Appl.*, 2016, pp. 1–4.

[176] D. Johannesson, M. Nawaz, and K. Ilves, "Assessment of 10 kV, 100 A silicon carbide MOSFET power modules," *IEEE Trans. Power Electron.*, vol. 33, no. 6, pp. 5215–5225, Jun. 2018.

[177] A. B. Jørgensen et al., "Reduction of parasitic capacitance in 10kV SiC MOSFET power modules using 3D FEM," in *2017 19th Eur. Conf. Power Electron. Appl*. IEEE, 2017, pp. P-1–P-8.

[178] D. N. Dalal et al., "Impact of power module parasitic capacitances on medium-voltage SiC MOSFETs switching transients," *IEEE Trans. Emerg. Sel. Topics Power Electron.*, vol. 8, no. 1, pp. 298–310, Mar. 2020.

[179] M. Johnson et al., "10kV SiC power module packaging," in *Proc. CIPS 2018; 10th Int. Conf. Integr. Power Electron. Syst.*, VDE, 2018, pp. 1–8.

[180] C. DiMarino et al., "Design and experimental validation of a wire-bondless 10-kV SiC MOSFET power module," *IEEE Trans. Emerg. Sel. Topics Power Electron.*, vol. 8, no. 1, pp. 381–394, Mar. 2020.

[181] L. Ravi, X. Lin, D. Dong, and R. Burgos, "An 11 kV AC, 16 kV DC, 200 kW direct-to-line inverter building-block using series-connected 10 kV SiC MOSFETs," in *2020 IEEE Energy Convers. Congr. Expo.*, 2020, pp. 362–369.

[182] J. K. Jørgensen, D. N. Dalal, S. Bęczkowski, S. Munk-Nielsen, and C. Uhrenfeldt, "Multi-chip medium voltage SiC MOSFET power module with focus on low parasitic capacitance," in *Proc. CIPS 2020; 11th Int. Conf. Integr. Power Electron. Syst.*, 2020, pp. 1–6.

[183] B. Passmore and C. O'Neal, "High-voltage SiC power modules for 10–25kV applications," in *Power Electron. Europe Mag*, vol. 1, pp. 22–24, 2016.

[184] H. Lee, V. Smet, and R. Tummala, "A review of SiC power module packaging technologies: Challenges, advances, and emerging issues," *IEEE Trans. Emerg. Sel. Topics Power Electron.*, vol. 8, no. 1, pp. 239–255, Mar. 2020.

[185] C. Chen, F. Luo, and Y. Kang, "A review of SiC power module packaging: Layout, material system and integration," *CPSS Trans. Power Electron. Appl.*, vol. 2, no. 3, pp. 170–186, Sep. 2017.

[186] F. Hou et al., "Review of packaging schemes for power module," *IEEE Trans. Emerg. Sel. Topics Power Electron.*, vol. 8, no. 1, pp. 223–238, Mar. 2020.

[187] Rogers Corporation, "curamik metallized ceramic substrates," Accessed: Apr. 2024. [Online]. Available: https://www.rogerscorp.com/advanced-electronics-solutions/curamik-ceramic-substrates

[188] J. Lutz, "Packaging and reliability of power modules," in *Proc. CIPS 2014; 8th Int. Conf. Integr. Power Electron. Syst.*, 2014, pp. 1–8.

[189] A. L. M. T. Corp, "MAGSIC for IGBT modules used in electric railway," Accessed: Apr. 2024. [Online]. Available: https://www.allied-material.co.jp/en/research-development/heatspreader.html#hsdev01

[190] Stanford Advanced Materials, "AL1885 AlSiC aluminum silicon carbide IGBT base plate," Accessed: Apr. 2024. [Online]. Available: https://www.samaterials.com/aluminium/1885-alsic-aluminum-silicon-carbide-igbt-base-plate.html

[191] T. G. Lei, J. N. Calata, G.-Q. Lu, X. Chen, and S. Luo, "Low-temperature sintering of nanoscale silver paste for attaching large-area ($>100\text{mm}^2$) chips," *IEEE Trans. Compon. Packag. Technol.*, vol. 33, no. 1, pp. 98–104, Mar. 2010.

[192] M. Knoerr, S. Kraft, and A. Schletz, "Reliability assessment of sintered nano-silver die attachment for power semiconductors," in *2010 12th Electron. Packag. Technol. Conf.*, 2010, pp. 56–61.

[193] W. Schmitt and L. M. Chew, "Silver sinter paste for SiC bonding with improved mechanical properties," in *2017 IEEE 67th Electron. Compon. Technol. Conf.*, 2017, pp. 1560–1565.

[194] W. W. Sheng and R. P. Colino, *Power Electron. Modules: Des. and Manufacture*. Boca Raton, FL, USA: CRC Press, 2004. [Online]. Available: https://www.routledge.com/Power-Electronic-Modules-Design-and-Manufacture/Sheng-Colino/p/book/9780849322600

[195] G. Chen et al., "Reliability comparison between SAC305 joint and sintered nanosilver joint at high temperatures for power electronic packaging," *J. Mater. Process. Technol.*, vol. 214, no. 9, pp. 1900–1908, 2014.

[196] Heraeus, "Bonding wires for semiconductor technology," Sep. 2017. Accessed: Apr. 2024. [Online]. Available: https://www.heraeus.com/media/media/het/doc_het/products_and_solutions_het_documents/bonding_wires_documents/Brochure_Bonding_Wire.pdf

[197] N. Marenco, M. Kontek, W. Reinert, J. Lingner, and M.-H. Poech, "Copper ribbon bonding for power electronics applications," in *2013 Eur. Microelectronics Packag. Conf.*, 2013, pp. 1–4.

[198] S. Seal, M. D. Glover, A. K. Wallace, and H. A. Mantooth, "Flip-chip bonded silicon carbide MOSFETs as a low parasitic alternative to wire-bonding," in *2016 IEEE 4th Workshop Wide Bandgap Power Devices Appl.*, 2016, pp. 194–199.

[199] Z. Liang, F. Wang, and L. Tolbert, "Development of packaging technologies for advanced SiC power modules," in *2014 IEEE Workshop Wide Bandgap Power Devices Appl.*, 2014, pp. 42–47.

[200] I. Kasko, S. E. Berberich, M. Spang, and S. Oehling, "SiC MOS power module in direct pressed die technology and some challenges for implementation," in *2020 32nd Int. Symp. Power Semicond. Devices ICs*, 2020, pp. 364–367.

[201] M. Horio, Y. Iizuka, Y. Ikeda, E. Mochizuki, and Y. Takahashi, "Ultra compact and high reliable SiC MOSFET power module with 200°C operating capability," in *2012 24th Int. Symp. Power Semicond. Devices ICs*, 2012, pp. 81–84.

[202] F. F. Wang and Z. Zhang, "Overview of silicon carbide technology: Device, converter, system, and application," *CPSS Trans. Power Electron. Appl.*, vol. 1, no. 1, pp. 13–32, Dec. 2016.

[203] M. Yaakub et al., "Silicon carbide power device characteristics, applications and challenges: An overview," *Int. J. Power Electron. Drive Syst.*, vol. 11, pp. 2194–2202, 2020.

[204] M. Buffolo et al., "Review and outlook on GaN and SiC power devices: Industrial state-of-the-art, applications, and perspectives," *IEEE Trans. Electron Devices*, vol. 71, no. 3, pp. 1344–1355, Mar. 2024.

[205] D. Dong, X. Lin, L. Ravi, N. Yan, and R. Burgos, "Advancement of SiC high-frequency power conversion systems for medium-voltage high-power applications," in *2020 IEEE 9th Int. Power Electron. Motion Control Conf.*, 2020, pp. 717–724.

[206] J. Carrasco et al., "Power-electronic systems for the grid integration of renewable energy sources: A survey," *IEEE Trans. Ind. Electron.*, vol. 53, no. 4, pp. 1002–1016, Jun. 2006.

[207] A. I. Elsanabary, G. Konstantinou, S. Mekhilef, C. D. Townsend, M. Seyedmahmoudian, and A. Stojcevski, "Medium voltage large-scale grid-connected photovoltaic systems using cascaded H-bridge and modular multilevel converters: A review," *IEEE Access*, vol. 8, pp. 223686–223699, 2020.

[208] M. R. Islam, A. M. Mahfuz-Ur-Rahman, K. M. Muttaqi, and D. Sutanto, "State-of-the-art of the medium-voltage power converter technologies for grid integration of solar photovoltaic power plants," *IEEE Trans. Energy Convers.*, vol. 34, no. 1, pp. 372–384, Mar. 2019.

[209] E. Serban, M. Ordonez, and C. Pondiche, "DC-Bus voltage range extension in 1500 V photovoltaic inverters," *IEEE Trans. Emerg. Sel. Topics Power Electron.*, vol. 3, no. 4, pp. 901–917, Dec. 2015.

[210] E. Bellini, "Silicon-carbide inverter for medium-voltage grids," Jan. 2021. Accessed: Feb. 2024. [Online]. Available: https://www.pv-magazine.com/2021/01/25/silicon-carbide-inverter-for-medium-voltage-grids/

[211] Y. Zhao, "A reliable, cost-effective transformerless medium-voltage inverter for grid integration of combined solar and energy storage," Univ. Arkansas, Fayetteville, AR, USA, DOE Contract no. DE-EE0008349, Mar. 2022. Accessed: Mar. 2024. [Online]. Available: https://www.osti.gov/biblio/1865551

[212] Fraunhofer ISE, "MS-LeiKra–Powerelectronics for the Next generation of medium voltage PV power plants," Nov. 2023. Accessed: Feb. 2024. [Online]. Available: https://www.ise.fraunhofer.de/en/research-projects/ms-leikra.html

[213] Fraunhofer ISE, "World premiere: Fraunhofer ISE presents medium-voltage string inverter for photovoltaics," Oct. 2023. Accessed: Feb. 2024. [Online]. Available: https://www.ise.fraunhofer.de/en/press-media/press-releases/2023/world-premiere-fraunhofer-ise-presents-medium-voltage-string-inverter-for-photovoltaics.html

[214] E. A. Gunther, "The state of medium voltage DC architectures for utility-scale PV," Feb. 2018. Accessed: Feb. 2024. [Online]. Available: https://www.pv-tech.org/the-state-of-medium-voltage-dc-architectures-for-utility-scale-pv/

[215] R. Chattopadhyay et al., "Low voltage PV power integration into medium voltage grid using high voltage SiC devices," in *2014 Int. Power Electron. Conf.*, 2014, pp. 3225–3232.

[216] F. M. Alhuwaishel, A. K. Allehyani, S. A. S. Al-Obaidi, and P. N. Enjeti, "A medium-voltage DC-Collection grid for large-scale PV power plants with interleaved modular multilevel converter," *IEEE Trans. Emerg. Sel. Topics Power Electron.*, vol. 8, no. 4, pp. 3434–3443, Dec. 2020.

[217] S. K. Voruganti and G. Gohil, "SiC-Enabled medium voltage isolated DC-DC converter based power optimizer for large photovoltaic parks," in *2020 IEEE Appl. Power Electron. Conf. Expo.*, 2020, pp. 2265–2271.

[218] J. J. Attukadavil, S. Anand, and B. G. Fernandes, "An adaptive DC voltage control for SiC based medium voltage photovoltaic inverter," in *2022 IEEE Energy Convers. Congr. Expo.*, 2022, pp. 1–7.

[219] J. Thoma, D. Chilachava, and D. Kranzer, "A highly efficient DC-DC-converter for medium-voltage applications," in *Proc. IEEE Int. Energy Conf.*, 2014, pp. 127–131.

[220] T. Liu et al., "Design and implementation of high efficiency control scheme of dual active bridge based 10 kV/1 MW solid state transformer for PV application," *IEEE Trans. Power Electron.*, vol. 34, no. 5, pp. 4223–4238, May 2019.

[221] W. Xu, Z. Guo, A. Vetrivelan, R. Yu, and A. Q. Huang, "Hardware design of a 13.8-kV/3-MVA PV plus storage solid-state transformer (PVS-SST)," *IEEE Trans. Emerg. Sel. Topics Power Electron.*, vol. 10, no. 4, pp. 3571–3586, Aug. 2022.

[222] International Energy Agency, "Tripling renewable power capacity by 2030 is vital to keep the 1.5°C goal within reach," Jul. 2023. Accessed: Apr. 2024. [Online]. Available: https://www.iea.org/commentaries/tripling-renewable-power-capacity-by-2030-is-vital-to-keep-the-150c-goal-within-reach

[223] Goldwind, "Pioneering a green future with wind energy," Accessed: Apr. 2024. [Online]. Available: https://www.goldwind.com/en/windpower/

[224] ABB, "ABB wind turbine converters," Mar. 2014. Accessed: Sep. 2023. [Online]. Available: https://search.abb.com/library/Download.aspx?DocumentID=3AFE68756031&LanguageCode=en&DocumentPartId=1&Action=Launch

[225] Ingeteam, "Ingeteam develops medium voltage full power converter product range for up to 18MW offshore turbines," Nov. 2022. Accessed: Sep. 2023. [Online]. Available: https://www.ingeteam.com/br/Pressroom/tabid/3373/articleType/ArticleView/articleId/3442/language/en-US/Ingeteam-develops-medium-voltage-full-power-converter-product-range-for-up-to-18MW-offshore-turbines.aspx

[226] J. Wahlström, "A new generation of medium voltage wind converters holds the key to sustainable wind power," Jul. 2023. Accessed: Sep. 2023. [Online]. Available: https://www.windpowerengineering.com/a-new-generation-of-medium-voltage-wind-converters-holds-the-key-to-sustainable-wind-power/

[227] C. Dincan, P. Kjær, and L. Helle, "Cost of energy assessment of wind turbine configurations," in *2020 22nd Eur. Conf. Power Electron. Appl.*, 2020, pp. 1–8.

[228] R. Dey and S. Nath, "Replacing silicon IGBTs with SiC IGBTs in medium voltage wind energy conversion systems," in *2016 7th India Int. Conf. Power Electron.*, 2016, pp. 1–6.

[229] Y. Wu, K. Choksi, Mustafeez-Ul-Hassan, and F. Luo, "An application analysis of wide-bandgap device for medium voltage wind energy conversion system," in *2022 IEEE 13th Int. Symp. Power Electron. Distrib. Gener. Syst.*, 2022, pp. 1–6.

[230] W. L. Erdman, J. Keller, D. Grider, and E. VanBrunt, "A 2.3-MW medium-voltage, three-level wind energy inverter applying a unique bus structure and 4.5-kV Si/SiC hybrid isolated power modules," in *2015 IEEE Appl. Power Electron. Conf. Expo.*, 2015, pp. 1282–1289.

[231] D. N. Dalal et al., "Demonstration of a 10 kV SiC MOSFET based medium voltage power stack," in *2020 IEEE Appl. Power Electron. Conf. Expo.*, 2020, pp. 2751–2757.

[232] J. Jacobsen et al., "Test platform for comparative evaluation of 690 V–4160 V power electronic converters," in *2022 IEEE 13th Int. Symp. Power Electron. Distrib. Gener. Syst.*, 2022, pp. 1–8.

[233] W. Chen, A. Q. Huang, C. Li, G. Wang, and W. Gu, "Analysis and comparison of medium voltage high power DC/DC converters for offshore wind energy systems," *IEEE Trans. Power Electron.*, vol. 28, no. 4, pp. 2014–2023, Apr. 2013.

[234] T. Lagier, P. Ladoux, and P. Dworakowski, "Potential of silicon carbide MOSFETs in the DC/DC converters for future HVDC offshore wind farms," *High Voltage*, vol. 2, no. 4, pp. 233–243, 2017.

[235] M. R. Nielsen, M. Kjær, H. Zhao, M. M. Bech, and S. Munk-Nielsen, "Closed-loop current control of a three-phase, two-level medium voltage power converter enabled by 10 kV SiC MOSFETs," in *Proc. IEEE 10th Int. Power Electron. Motion Control Conf.*, Chengdu, China, 2024, pp. 1256–1260.

[236] X. She, A. Q. Huang, and R. Burgos, "Review of solid-state transformer technologies and their application in power distribution systems," *IEEE Trans. Emerg. Sel. Topics Power Electron.*, vol. 1, no. 3, pp. 186–198, Sep. 2013.

[237] H. Mhiesan, Y. Wei, Y. P. Siwakoti, and H. A. Mantooth, "A fault-tolerant hybrid cascaded H-bridge multilevel inverter," *IEEE Trans. Power Electron.*, vol. 35, no. 12, pp. 12702–12715, Dec. 2020.

[238] R. Chen et al., "10 kV SiC MOSFET based medium voltage power conditioning system for asynchronous microgrids," *IEEE Access*, vol. 10, pp. 73294–73308, 2022.

[239] S. Madhusoodhanan et al., "Comparative evaluation of 15 kV SiC IGBT and 15 kV SiC MOSFET for 3-phase medium voltage high power grid connected converter applications," in *2016 IEEE Energy Convers. Congr. Expo.*, 2016, pp. 1–8.

[240] S. Parashar, A. Kumar, and S. Bhattacharya, "High power medium voltage converters enabled by high voltage SiC power devices," in *2018 Int. Power Electron. Conf.*, 2018, pp. 3993–4000.

[241] R. K. Kokkonda, S. Parashar, and S. Bhattacharya, "Performance comparison of 10 kV and series-connected 3.3 kV SiC MOSFETs based VSCs for MV grid interfacing applications," in *2023 IEEE Appl. Power Electron. Conf. Expo.*, 2023, pp. 995–1002.

[242] F. Wang and H. Li, "Survey and benchmark of benefits of high voltage SiC applications in medium voltage power distribution grids," Oak Ridge Nat. Lab., Oak Ridge, TN, USA, Tech. Rep. ORNL/TM-2022/2561, 2022. [Online]. Available: https://www.osti.gov/biblio/1922316

[243] H. Li, Y. Ma, R. Ren, and F. Wang, "SiC impact on grid power electronics converters," in *2020 IEEE Power Energy Soc. Gen. Meeting*, 2020, pp. 1–5.

[244] A. Anurag, S. Acharya, N. Kolli, S. Bhattacharya, T. R. Weatherford, and A. A. Parker, "A three-phase active-front-end converter system enabled by 10-kV SiC MOSFETs aimed at a solid-state transformer application," *IEEE Trans. Power Electron.*, vol. 37, no. 5, pp. 5606–5624, May 2022.

[245] A. Anurag, S. Acharya, S. Bhattacharya, T. R. Weatherford, and A. A. Parker, "A Gen-3 10-kV SiC MOSFET-based medium-voltage three-phase dual active bridge converter enabling a mobile utility support equipment solid state transformer," *IEEE Trans. Emerg. Sel. Topics Power Electron.*, vol. 10, no. 2, pp. 1519–1536, Apr. 2022.

[246] S. Madhusoodhanan et al., "Solid-state transformer and MV grid tie applications enabled by 15 kV SiC IGBTs and 10 kV SiC MOSFETs based multilevel converters," *IEEE Trans. Ind. Appl.*, vol. 51, no. 4, pp. 3343–3360, Jul./Aug. 2015.

[247] K. Mainali et al., "A transformerless intelligent power substation: A three-phase SST enabled by a 15-kV SiC IGBT," *IEEE Power Electron. Mag.*, vol. 2, no. 3, pp. 31–43, Sep. 2015.

[248] S. Ji et al., "Medium voltage (13.8 kV) transformer-less grid-connected DC/AC converter design and demonstration using 10 kV SiC MOSFETs," in *2019 IEEE Energy Convers. Congr. Expo.*, 2019, pp. 1953–1959.

[249] R. Chen et al., "Design of 10 kV SiC MOSFET power module based MW-level modular multilevel converter phase-leg," in *2024 IEEE Appl. Power Electron. Conf. Expo.*, 2024, pp. 1087–1094.

[250] R. Chen et al., "Switching cell design for medium voltage flying capacitor converter with 10 kV SiC MOSFET," in *2024 IEEE Appl. Power Electron. Conf. Expo.*, 2024, pp. 2468–2474.

[251] F. Wang, G. Wang, A. Huang, W. Yu, and X. Ni, "Design and operation of a 3.6 kV high performance solid state transformer based on 13 kV SiC MOSFET and JBS diode," in *2014 IEEE Energy Convers. Congr. Expo.*, 2014, pp. 4553–4560.

[252] D. Rothmund, T. Guillod, D. Bortis, and J. W. Kolar, "99.1% efficient 10 kV SiC-Based medium-voltage ZVS bidirectional single-phase PFC AC/DC stage," *IEEE Trans. Emerg. Sel. Topics Power Electron.*, vol. 7, no. 2, pp. 779–797, Jun. 2019.

[253] A. Q. Huang, Q. Zhu, L. Wang, and L. Zhang, "15 kV SiC MOSFET: An enabling technology for medium voltage solid state transformers," *CPSS Trans. Power Electron. Appl.*, vol. 2, no. 2, pp. 118–130, 2017.

[254] Q. Zhu, L. Wang, D. Chen, L. Zhang, and A. Q. Huang, "Design and implementation of a 7.2 kV single stage AC-AC solid state transformer based on current source series resonant converter and 15 kV SiC MOSFET," in *2017 IEEE Energy Convers. Congr. Expo.*, 2017, pp. 1288–1295.

[255] A. H. Wijenayake et al., "Next-generation MVDC architecture based on 6.5 kV / 200 A, 12.5 mΩ SiC H-bridge and 10 kV / 240 A, 20 mΩ SiC dual power modules," in *2017 IEEE Electric Ship Technol. Symp.*, 2017, pp. 598–604.

[256] L. Zheng, R. P. Kandula, and D. Divan, "Soft-switching solid-state transformer with reduced conduction loss," *IEEE Trans. Power Electron.*, vol. 36, no. 5, pp. 5236–5249, May 2021.

[257] L. Zheng et al., "7.2 kV three-port SiC single-stage current-source solid-state transformer with 90 kV lightning protection," *IEEE Trans. Power Electron.*, vol. 37, no. 10, pp. 12080–12094, Oct. 2022.

[258] N. Kolli, S. Parashar, R. K. Kokkonda, S. Bhattacharya, and V. Veliadis, "Design of asynchronous microgrid power conditioning system with Gen-3 10 kV SiC MOSFETs for MV grid interconnection," in *2024 IEEE Appl. Power Electron. Conf. Expo.*, 2024, pp. 514–521.

[259] R. A. Gomez, D. A. Porras, G. G. Oggier, J. C. Balda, and Y. Zhao, "A three-phase isolated building block for high-power medium-voltage grid applications," *IEEE Trans. Emerg. Sel. Topics Power Electron.*, vol. 12, no. 2, pp. 1324–1336, Apr. 2024.

[260] R. W. D. Doncker, "The war of currents," EE Online, Jul. 2020. Accessed: Mar. 2024. [Online]. Available: https://electricenergyonline.com/energy/magazine/1276/article/the-war-of-currents.htm

[261] A. Maitra, "Utility direct medium voltage DC fast charger update: DC fast charger characterization," EPRI, Dec. 2012. Accessed: Feb. 2024. [Online]. Available: https://www.epri.com/research/products/1024106

[262] C. Zhu, "High-efficiency, medium-voltage input, solid-state, Transformer based 400-kW/1000-V/400-A extreme fast charger for electric vehicles," Delta Electronics, Award no. DE-EE0008361 - ELT241, Nov. 2021. Accessed: Feb. 2024. [Online]. Available: https://www.energy.gov/eere/vehicles/articles/high-efficiency-medium-voltage-input-solid-state-transformer-based-400

[263] S. Lukic, "Intelligent, grid-friendly, modular extreme fast charging system with solid-state DC protection," North Carolina State Univ., Raleigh, NC, USA, Award no. DE-EE0008450 - ELT238, Dec. 2021. Accessed: Feb. 2024. [Online]. Available: https://www.energy.gov/eere/vehicles/articles/intelligent-grid-friendly-modular-extreme-fast-charging-system-solid-state-1

[264] S. Bhattacharya, "Low-cost compact medium voltage connected DC charging infrastructure," Aug. 2023. Accessed: Feb. 2024. [Online]. Available: https://ece.ncsu.edu/grant/low-cost-compact-medium-voltage-connected-dc-charging-infrastructure/

[265] K. Wijnands, "Medium-voltage fast charging," 2022. Accessed: Feb. 2024. [Online]. Available: https://neonresearch.nl/work_package/medium-voltage-fast-charging/

[266] M. U. Mutarraf et al., "Electric cars, ships, and their charging infrastructure–A. comprehensive review," *Sustain. Energy Technol. Assessments*, vol. 52, 2022, Art. no. 102177. [Online]. Available: https://www.sciencedirect.com/science/article/pii/S2213138822002296

[267] S. Srdic and S. Lukic, "Toward extreme fast charging: Challenges and opportunities in directly connecting to medium-voltage line," *IEEE Electrific. Mag.*, vol. 7, no. 1, pp. 22–31, Mar. 2019.

[268] H. Tu, H. Feng, S. Srdic, and S. Lukic, "Extreme fast charging of electric vehicles: A technology overview," *IEEE Trans. Transport. Electrific.*, vol. 5, no. 4, pp. 861–878, Dec. 2019.

[269] S. Li, S. Lu, and C. C. Mi, "Revolution of electric vehicle charging technologies accelerated by wide bandgap devices," *Proc. IEEE Proc. IRE*, vol. 109, no. 6, pp. 985–1003, Jun. 2021.

[270] S. Rivera, S. Kouro, S. Vazquez, S. M. Goetz, R. Lizana, and E. Romero-Cadaval, "Electric vehicle charging infrastructure: From grid to battery," *IEEE Ind. Electron. Mag.*, vol. 15, no. 2, pp. 37–51, Jun. 2021.

[271] B. Shi et al., "A review of silicon carbide MOSFETs in electrified vehicles: Application, challenges, and future development," *IET Power Electron.*, vol. 16, no. 12, pp. 2103–2120, 2023, doi: 10.1049/pel2.12524.

[272] X. Liang, S. Srdic, J. Won, E. Aponte, K. Booth, and S. Lukic, "A 12.47 kV medium voltage input 350 kW EV fast charger using 10 kV SiC MOSFET," in *2019 IEEE Appl. Power Electron. Conf. Expo.*, 2019, pp. 581–587.

[273] L. Gill, T. Ikari, T. Kai, B. Li, K. Ngo, and D. Dong, "Medium voltage dual active bridge using 3.3 kV SiC MOSFETs for EV charging application," in *2019 IEEE Energy Convers. Congr. Expo.*, 2019, pp. 1237–1244. [Online]. Available: https://api.semanticscholar.org/CorpusID:208629819

[274] M. A. Awal et al., "Medium voltage solid state transformer for extreme fast charging applications," in *2023 IEEE Appl. Power Electron. Conf. Expo.*, 2023, pp. 1528–1535.

[275] Siemens AG, "Megawatt charging system from siemens delivers 1 MW charge for the first-time during testing," Apr. 2024. Accessed: Apr. 2024. [Online]. Available: https://press.siemens.com/global/en/pressrelease/megawatt-charging-system-siemens-delivers-1-mw-charge-first-time-during-testing?linkId=300000011141076

[276] Transport and Environment, "Electrofuels? Yes, we can... if we are efficient," Dec. 2020. Accessed: Feb. 2024. [Online]. Available: https://www.transportenvironment.org/wp-content/uploads/2020/12/2020_12_Briefing_feasibility_study_renewables_decarbonisation.pdf

[277] B. Hinman, "Aircraft charging unit," Sep. 2022. Accessed: Feb. 2024. [Online]. Available: https://brian-is-flyin.medium.com/aircraft-charging-unit-80369c555ef0

[278] EE Power, "High-voltage charger to propel hybrid-electric aircraft demonstrator," Feb. 2024. Accessed: Feb. 2024. [Online]. Available: https://eepower.com/news/high-voltage-charger-to-propel-hybrid-electric-aircraft-demonstrator/

[279] Emobility Engineering, "ABB plans fast-charger network for electric aircraft," 2021. Accessed: Feb. 2024. [Online]. Available: https://www.emobility-engineering.com/abb-plans-fast-charger-network-for-electric-aircraft/

[280] Airbus, "Airbus' high-voltage battery technology," Mar. 2022. Accessed: Feb. 2024. [Online]. Available: https://www.airbus.com/en/newsroom/news/2022-03-airbus-high-voltage-battery-technology-prepares-for-ecopulse-flight-test

[281] J. Park et al., "Electric aircraft battery with high voltage (800 V) modular design," 2022. Accessed: Feb. 2024. [Online]. Available: https://www.nasa.gov/wp-content/uploads/2024/01/optimizing-for-power-and-safety-electric-aircraft-battery-withhigh-voltage-800v-modular-design.pdf?emrc=65d06322de4ed

[282] Aerospace Manufacturing, "Pratt & Whitney unveils high voltage bidirectional mobile charging unit for hybrid-electric flight," Jan. 2024. Accessed: Mar. 2024. [Online]. Available: https://www.aero-mag.com/pratt-whitney-unveils-high-voltage-bidirectional-mobile-charging-unit-for-hybrid-electric-flight

[283] K. M. U. Ahmed, M. H. J. Bollen, and M. Alvarez, "A review of data centers energy consumption and reliability modeling," *IEEE Access*, vol. 9, pp. 152536–152563, 2021.

[284] R. Turner and N. Elliott, "A new UPS topology for multi-megawatt medium voltage power protection," in *2018 IEEE Int. Conf. Ind. Electron. Sustain. Energy Syst.*, 2018, pp. 245–249.

[285] G. AlLee and W. Tschudi, "Edison Redux: 380 Vdc brings reliability and efficiency to sustainable data centers," *IEEE Power Energy Mag.*, vol. 10, no. 6, pp. 50–59, Nov./Dec. 2012.

[286] S. Zhao, Q. Li, F. C. Lee, and B. Li, "High-frequency transformer design for modular power conversion from medium-voltage AC to 400 VDC," *IEEE Trans. Power Electron.*, vol. 33, no. 9, pp. 7545–7557, Sep. 2018.

[287] D. Rothmund, T. Guillod, D. Bortis, and J. W. Kolar, "99% efficient 10 kV SiC-Based 7 kV/400 V DC transformer for future data centers," *IEEE Trans. Emerg. Sel. Topics Power Electron.*, vol. 7, no. 2, pp. 753–767, Jun. 2019.

[288] J. E. Huber, J. Böhler, D. Rothmund, and J. W. Kolar, "Analysis and cell-level experimental verification of a 25 kW all-SiC isolated front end 6.6 kV/400 V AC-DC solid-state transformer," *CPSS Trans. Power Electron. Appl.*, vol. 2, no. 2, pp. 140–148, 2017.

[289] S. Acharya et al., "High power medium voltage 10 kV SiC MOSFET based bidirectional isolated modular DC–DC converter," in *2018 Int. Power Electron. Conf.*, 2018, pp. 3564–3571.

[290] X. Du, Z. Ma, M. Jiang, A. Ismail, and Y. Zhao, "Characterizations and converter design using the latest 6.5 kV silicon carbide MOSFETs," in *2024 IEEE Appl. Power Electron. Conf. Expo.*, 2024, pp. 3140–3144.

[291] ABB, "Hydrogen production," Apr. 2022. Accessed: Feb. 2024. [Online]. Available: https://new.abb.com/news/detail/96198/hydrogen-production

[292] J. Solanki et al., "High-current variable-voltage rectifiers: State of the art topologies," *IET Power Electron.*, vol. 8, no. 6, pp. 1068–1080, 2015, doi: 10.1049/iet-pel.2014.0533.

[293] R. Mirzadarani et al., "Three-phase medium-voltage medium-frequency transformer for SST in green hydrogen production," in *Proc. 49th Annu. Conf. Ind. Electron. Soc. Conf.*, 2023, pp. 1–6.

[294] Z. Yan et al., "Light-load performance comparison of medium-voltage isolated DC-DC converters enabled by 10 kV SiC MOSFETs," in *Proc. IEEE 10th Int. Power Electron. Motion Control Conf.*, Chengdu, China, 2024, pp. 1708–1712.

[295] W. Zhao, M. R. Nielsen, M. Kjær, F. Iov, and S. M. Nielsen, "Grid integration of a 500 kW alkaline electrolyzer system for harmonic analysis and robust control," *e-Prime -Adv. Elect. Eng., Electron. Energy*, vol. 5, 2023, Art. no. 100217. [Online]. Available: https://www.sciencedirect.com/science/article/pii/S2772671123001122

[296] H. Abu-Rub, S. Bayhan, S. Moinoddin, M. Malinowski, and J. Guzinski, "Medium-voltage drives: Challenges and existing technology," *IEEE Power Electron. Mag.*, vol. 3, no. 2, pp. 29–41, Jun. 2016.

[297] F. Bartos, "Why choose medium-voltage drives?," in *Control Eng. - Highlands Ranch- Cahners Then Reed Bus. Inf.-*, vol. 64, pp. 52–55, 2010.

[298] A. Marzoughi, R. Burgos, and D. Boroyevich, "Investigating impact of emerging medium-voltage SiC MOSFETs on medium-voltage high-power industrial motor drives," *IEEE Trans. Emerg. Sel. Topics Power Electron.*, vol. 7, no. 2, pp. 1371–1387, Jun. 2019.

[299] S. Madhusoodhanan, K. Mainali, A. Tripathi, K. Vechalapu, and S. Bhattacharya, "Medium voltage ($\geq$2.3 kV) high frequency three-phase two-level converter design and demonstration using 10 kV SiC MOSFETs for high speed motor drive applications," in *2016 IEEE Appl. Power Electron. Conf. Expo.*, 2016, pp. 1497–1504.

[300] F. Kieferndorf, M. Basler, L. A. Serpa, J.-H. Fabian, A. Coccia, and G. A. Scheuer, "ANPC-5L technology applied to medium voltage variable speed drives applications," in *Proc. SPEEDAM 2010*, 2010, pp. 1718–1725.

[301] X. Song, A. Q. Huang, X. Ni, and L. Zhang, "Comparative evaluation of 6 kV Si and SiC power devices for medium voltage power electronics applications," in *2015 IEEE 3rd Workshop Wide Bandgap Power Devices Appl.*, 2015, pp. 150–155.

[302] A. Marzoughi, R. Burgos, D. Boroyevich, and Y. Xue, "Design and comparison of cascaded H-bridge, modular multilevel converter, and 5-L active neutral point clamped topologies for motor drive applications," *IEEE Trans. Ind. Appl.*, vol. 54, no. 2, pp. 1404–1413, Mar./Apr. 2018.

[303] M. Adamowicz and J. Szewczyk, "SiC-based power electronic traction transformer (PETT) for 3 kV DC rail traction," *Energies*, vol. 13, no. 21, 2020, Art. no. 5573. [Online]. Available: https://www.mdpi.com/1996-1073/13/21/5573

[304] A. Morya, M. Moosavi, M. C. Gardner, and H. A. Toliyat, "Applications of wide bandgap (WBG) devices in AC electric drives: A technology status review," in *2017 IEEE Int. Electric Mach. Drives Conf.*, 2017, pp. 1–8.

[305] J. Pan et al., "7-kV 1-MVA SiC-based modular multilevel converter prototype for medium-voltage electric machine drives," *IEEE Trans. Power Electron.*, vol. 35, no. 10, pp. 10137–10149, Oct. 2020.

[306] R. K. Kokkonda, S. Parashar, P. P. Das, and S. Bhattacharya, "A 6.5 kV SiC MOSFET based inverter for medium voltage (2.3 kV) high-speed motor drive applications," in *2023 IEEE Energy Convers. Congr. Expo.*, 2023, pp. 4660–4667.

[307] R. K. Kokkonda and S. Bhattacharya, "Soft switching ARCP inverter using series connected SiC MOSFETs for medium voltage motor drive applications," in *2024 IEEE Appl. Power Electron. Conf. Expo.*, 2024, pp. 567–574.

[308] G. Fortes, P. Ladoux, J. Fabre, and D. Flumian, "Characterization of a 300 kW isolated DCDC converter using 3.3 kV SiC-MOSFETs," in *Proc. PCIM Europe Digit. days 2021; Int. Exhib. Conf. Power Electron., Intell. Motion, Renewable Energy Energy Manage.*, 2021, pp. 1–8.

[309] P. Shenoy, O. Solis, and L. Zheng, "Commercializing medium voltage VFD that utilizes high voltage SiC technology," in *2017 IEEE Int. Workshop Integr. Power Packag.*, 2017, pp. 1–4.

[310] P. Shenoy and O. Solis, "Medium voltage integrated drive and motor," Calnetix Technologies, Contract no. DE-EE0007251, Jun. 2019. Accessed: Jun. 2024. [Online]. Available: https://www.energy.gov/sites/prod/files/2019/07/f65/Projects19%20-%20Medium%20Voltage%20Integrated%20Drive%20and%20Motor_Calnetix.pdf

[311] F. Diao et al., "A megawatt-scale Si/SiC hybrid multilevel inverter for electric aircraft propulsion applications," *IEEE Trans. Emerg. Sel. Topics Power Electron.*, vol. 11, no. 4, pp. 4095–4107, Aug. 2023.

[312] M. S. Diab and X. Yuan, "A modular quasi-multilevel converter using 10 kV SiC MOSFETs for medium-voltage cable-fed variable-speed motor drives," in *2021 IEEE 12th Energy Convers. Congr. Expo. - Asia*, 2021, pp. 781–786.

[313] Y. Zhang, R. Agarwal, and H. Li, "Active reflected wave canceller with partial discharge suppression for MV SiC motor drive," in *2022 IEEE Appl. Power Electron. Conf. Expo.*, 2022, pp. 809–812.

[314] P. Gammon, A. B. Renz, and G. Baker, "SiC power electronics: Looking beyond automotive," May 2022. Accessed: Mar. 2024. [Online]. Available: https://www.powerelectronicsnews.com/sic-power-electronics-looking-beyond-automotive/

[315] Power America, "PowerAmerica device bank bare die available for purchase," Aug. 2021. Accessed: Mar. 2024. [Online]. Available: https://poweramericainstitute.org/wp-content/uploads/2021/08/Device-Bank-Bare-Die-Inventory-website.pdf

[316] Power America, "PowerAmerica device bank bare die available for purchase," Accessed: Mar. 2024. [Online]. Available: https://poweramericainstitute.org/devicebank/wolfspeed-engineering-samples/

[317] United States of America, "H.R.4346 — CHIPS and science act," 2022. Accessed: Apr. 2024. [Online]. Available: https://www.congress.gov/bill/117th-congress/house-bill/4346

[318] European Union, "The European chips act," 2022, Accessed: Apr. 2024. [Online]. Available: https://www.european-chips-act.com/

[319] M. Fotopoulou et al., "State of the art of low and medium voltage direct current (DC) microgrids," *Energies*, vol. 14, no. 18, 2021, Art. no. 5595. [Online]. Available: https://www.mdpi.com/1996-1073/14/18/5595

[320] B. F. Kjærsgaard et al., "Parasitic capacitive couplings in medium voltage power electronic systems: An overview," *IEEE Trans. Power Electron.*, vol. 38, no. 8, pp. 9793–9817, Aug. 2023.

[321] A. B. Jørgensen et al., "Reduction of parasitic capacitance in 10 kV SiC MOSFET power modules using 3D FEM," in *2017 19th Eur. Conf. Power Electron. Appl.*, 2017, pp. P.1–P.8.

[322] C. M. DiMarino, B. Mouawad, C. M. Johnson, D. Boroyevich, and R. Burgos, "10-kV SiC MOSFET power module with reduced common-mode noise and electric field," *IEEE Trans. Power Electron.*, vol. 35, no. 6, pp. 6050–6060, Jun. 2020.

[323] H. Zhao et al., "Physics-based modeling of parasitic capacitance in medium-voltage filter inductors," *IEEE Trans. Power Electron.*, vol. 36, no. 1, pp. 829–843, Jan. 2021.

[324] H. Li, Z. Gao, and F. Wang, "Medium-voltage isolated auxiliary power supply design for high insulation capability, ultra-low coupling capacitance, and small size," *IEEE Trans. Power Electron.*, vol. 38, no. 6, pp. 7226–7240, Jun. 2023.

[325] M. R. Nielsen, M. Kirkeby, H. Zhao, D. N. Dalal, M. M. Bech, and S. Munk-Nielsen, "Noise analysis of current sensor for medium voltage power converter enabled by silicon-carbide MOSFETs," in *2022 IEEE 9th Workshop Wide Bandgap Power Devices Appl.*, 2022, pp. 180–185.

[326] R. Chen et al., "Analysis of 10 kV SiC MOSFET module baseplate parasitic capacitance impact on switching loss," in *2023 IEEE 10th Workshop Wide Bandgap Power Devices Appl.*, 2023, pp. 1–6.

[327] A. Deshpande and F. Luo, "Practical design considerations for a Si IGBT+SiC MOSFET hybrid switch: Parasitic interconnect influences, cost, and current ratio optimization," *IEEE Trans. Power Electron.*, vol. 34, no. 1, pp. 724–737, Jan. 2019.

[328] A. I. Emon, Z. Yuan, A. B. Mirza, A. Deshpande, M. U. Hassan, and F. Luo, "1200 V/650 V/160 A SiC si IGBT 3L hybrid T-type NPC power module with enhanced EMI shielding," *IEEE Trans. Power Electron.*, vol. 36, no. 12, pp. 13660–13673, Dec. 2021.

[329] Z. Zhang, Q. Yuchi, F. Boshkovski, K. D. Ngo, and G.-Q. Lu, "Field-grading effect of a nonlinear resistive polymer-nanoparticle composite triple-point coating on direct-bond copper substrates for packaging medium-voltage power devices," in *2022 IEEE Elect. Insul. Conf.*, 2022, pp. 439–442.

[330] B. Zhang, M. Ghassemi, and Y. Zhang, "Insulation materials and systems for power electronics modules: A review identifying challenges and future research needs," *IEEE Trans. Dielectr. Electr. Insul.*, vol. 28, no. 1, pp. 290–302, Feb. 2021.

[331] X. Li, Y. Chen, H. Chen, R. Paul, X. Song, and H. A. Mantooth, "A 10 kV SiC MOSFET power module with optimized system interface and electric field distribution," in *IEEE Trans. Power Electron.*, vol. 39, no. 8, pp. 9540–9553, Aug. 2024.

[332] P. Sun et al., "A comprehensive study on electric field coupling effects of medium-voltage SiC power module and optimization design," in *2024 IEEE Appl. Power Electron. Conf. Expo.*, 2024, pp. 2556–2561.

[333] H. Li, P. Yao, Z. Gao, and F. Wang, "Medium voltage converter inductor insulation design considering grid requirements," *IEEE Trans. Emerg. Sel. Topics Power Electron.*, vol. 10, no. 2, pp. 2339–2350, Apr. 2022.

[334] K. Sun, Y. Xu, J. Wang, R. Burgos, and D. Boroyevich, "Insulation design of wireless auxiliary power supply for medium voltage converters," *IEEE Trans. Emerg. Sel. Topics Power Electron.*, vol. 9, no. 4, pp. 4200–4211, Aug. 2021.

[335] C. Zhang, Y. Xu, M. Dong, R. Burgos, M. Ren, and D. Boroyevich, "Design and assessment of external insulation for critical components in a medium voltage SiC-Based converter via optical method," *IEEE Trans. Power Electron.*, vol. 35, no. 12, pp. 12887–12897, Dec. 2020.

[336] H. You, Z. Wei, B. Hu, Z. Zhao, R. Na, and J. Wang, "Partial discharge behaviors in power modules under square pulses with ultrafast dv/dt," *IEEE Trans. Power Electron.*, vol. 36, no. 3, pp. 2611–2620, Mar. 2021.

[337] Y. Ding, Y. Wang, H. Sun, and Y. Yin, "High-temperature partial discharge characteristics of power module packaging insulation under square pulse with high dv/dt based on down-mixing method," *IEEE Trans. Ind. Electron.*, vol. 70, no. 7, pp. 7334–7342, Jul. 2023.

[338] H. Li, S. Zhao, X. Wang, L. Ding, and H. A. Mantooth, "Parallel connection of silicon carbide MOSFETs—Challenges, mechanism, and solutions," *IEEE Trans. Power Electron.*, vol. 38, no. 8, pp. 9731–9749, Aug. 2023.

[339] D. Jin, N. Qi, J. Ouyang, and C. Luo, "Analysis and reduction of turn-on gate-source voltage oscillation on paralleled SiC MOSFETs application," in *2022 IEEE Energy Convers. Congr. Expo.*, 2022, pp. 1–7.

[340] F. Sawallich and H.-G. Eckel, "Inter-chip oscillation of paralleled SiC MOSFETs," in *Proc. PCIM Europe 2023; Int. Exhib. Conf. Power Electron., Intell. Motion, Renewable Energy Energy Manage.*, 2023, pp. 1–7.

[341] F. Sawallich and H.-G. Eckel, "Mitigating inter-chip oscillation of paralleled SiC MOSFETs," in *2023 25th Eur. Conf. Power Electron. Appl.*, 2023, pp. 1–11.

[342] B. F. Kjærsgaard et al., "Analysis of miller region sustained oscillations during turn-on of high-side 10 kV SiC MOSFET," in *2023 25th Eur. Conf. Power Electron. Appl.*, 2023, pp. 1–8.

[343] R. Wang, A. B. Jørgensen, D. N. Dalal, S. Luan, H. Zhao, and S. Munk-Nielsen, "Integrating 10-kV SiC MOSFET into battery energy storage system with a scalable converter-based self-powered gate driver," *IEEE Trans. Emerg. Sel. Topics Power Electron.*, vol. 11, no. 1, pp. 351–360, Feb. 2023.

[344] A. Kadavelugu, S. Bhattacharya, S.-H. Ryu, D. Grider, S. Leslie, and K. Hatua, "Understanding dv/dt of 15 kV SiC N-IGBT and its control using active gate driver," in *2014 IEEE Energy Convers. Congr. Expo.*, 2014, pp. 2213–2220.

[345] A. Tripathi, K. Mainali, S. Madhusoodhanan, A. Yadav, K. Vechalapu, and S. Bhattacharya, "A MV intelligent gate driver for 15 kV SiC IGBT and 10 kV SiC MOSFET," in *2016 IEEE Appl. Power Electron. Conf. Expo.*, 2016, pp. 2076–2082.

[346] Y. He, X. Wang, S. Shao, and J. Zhang, "Active gate driver for dynamic current balancing of parallel-connected SiC MOSFETs," *IEEE Trans. Power Electron.*, vol. 38, no. 5, pp. 6116–6127, May 2023.

[347] G. L. Rødal and D. Peftitsis, "Gate-drive circuits for adaptive operation of SiC MOSFETs," *IEEE Trans. Power Electron.*, vol. 39, no. 7, pp. 8162–8186, Jul. 2024.

[348] J. Gottschlich, M. Schäfer, M. Neubert, and R. W. De Doncker, "A galvanically isolated gate driver with low coupling capacitance for medium voltage SiC MOSFETs," in *2016 18th Eur. Conf. Power Electron. Appl.*, 2016, pp. 1–8.

[349] D. N. Dalal et al., "Gate driver with high common mode rejection and self turn-on mitigation for a 10 kV SiC MOSFET enabled MV converter," in *2017 19th Eur. Conf. Power Electron. Appl.*, 2017, pp. P.1–P.10.

[350] H. Zhao et al., "Modeling and design of a 1.2 pF common-mode capacitance transformer for powering MV SiC MOSFETs gate drivers," in *Proc. IECON 2019-45th Annu. Conf. IEEE Ind. Electron. Soc.*, 2019, pp. 5147–5153, vol. 1.

[351] Z. Guo and H. Li, "A fiber-optic-less 50-MHz single transformer isolated gate driver with fault feedback for 10-kV SiC MOSFETs," *IEEE Trans. Ind. Electron.*, vol. 71, no. 9, pp. 10854–10863, Sep. 2024.

Morten Rahr Nielsen (Graduate Student Member, IEEE) received the B.Sc. degree in electrical energy technology from Aarhus University, Aarhus, Denmark, in 2020, and the M.Sc. degree in energy engineering, with a specialization in power electronics and drives, from AAU Energy, Aalborg University, Aalborg, Denmark, in 2022.

He is currently a Research Assistant with AAU Energy, Aalborg University. His research interests include wide bandgap semiconductor devices and control of medium voltage, high-power converters.

Shiyue Deng (Graduate Student Member, IEEE) received the B.Sc. degree from Jiangsu University, Zhenjiang, China, in 2020, and the M.Sc. degree from Stony Brook University, Stony Brook, NY, USA, in 2022, both in electrical engineering. He is currently working toward the Ph.D. degree in electrical engineering with Stony Brook University.

His research interests include high-voltage power module packaging and high-power-density converter design.

Abdul Basit Mirza (Graduate Student Member, IEEE) received the B.Sc. (Hons.) degree in electrical engineering (power) from the University of Engineering and Technology, Lahore, Pakistan, in 2018, and the M.Sc. and Ph.D. degrees in electrical engineering from Stony Brook University, Stony Brook, NY, USA, in 2022 and 2024, respectively.

He is currently a Power Electronics Lead Engineer with Eaton Research Lab, Menomonee Falls, WI, USA. In 2022, he was a Research Intern with GE Global Research, Niskayuna, NY, USA. His research interests include system-level design and packaging of high-density and high-power converters, side effects (EMI/EMC, partial discharge, and high-frequency interactions) modeling and mitigation, integrated magnetics design, and noninvasive health monitoring of power converters using digital twin.

Benjamin Futtrup Kjærsgaard (Graduate Student Member, IEEE) received the Ph.D. degree in energy engineering from AAU Energy, Aalborg University, Aalborg, Denmark, in 2024.

He is currently a Power Electronics Designer with PowerCon A/S, Hobro, Denmark. His research interests include high-power medium-voltage power converter systems and designs, wide bandgap semiconductor devices, their switching dynamics, and the intracomponent impact of parasitic capacitive and inductive couplings.

Asger Bjørn Jørgensen received the M.Sc. and Ph.D. degrees in energy engineering from Aalborg University, Aalborg, Denmark, in 2016 and 2019, respectively.

He is currently an Assistant Professor with AAU Energy, Aalborg University. In 2018, he was a Visiting Researcher with FREEDM Systems Center, North Carolina State University, Raleigh, NC, USA. His research interests include integrated power module packaging, wide bandgap power semiconductors, and digital design optimization using multiphysics finite element simulation.

Dr. Bjørn Jørgensen was the recipient of the European Power Electronics and Drives Association (EPE) Outstanding Young EPE Member Award in 2020.

Hongbo Zhao (Member, IEEE) received the Ph.D. degree in energy engineering from AAU Energy, Aalborg University, Aalborg, Denmark, in 2021.

He is currently an Assistant Professor with AAU Energy, Aalborg University. He was a Visiting Researcher with the University of Texas at Austin, Austin, TX, USA, a Visiting Scholar with the University of Galway, Galway, Ireland, and a Visiting Professor with G2Elab, Grenoble, France. His research interests include analysis and packaging of modern magnetic components, as well as the applications of wide bandgap semiconductor devices.

Dr. Zhao is an Associate Editor for IEEE OPEN JOURNAL OF POWER ELECTRONICS. He was the recipient of the Villum Fellowship, in 2022. He was also the recipient of the "Best Magnetic Design" by Frenetic, in 2022. He was selected as a future entrepreneur by the Spin-outs Denmark program in 2023. His idea on next-generation sustainable magnetic components was awarded as "The Bright Idea Award" from Otto Mønsteds Fond in 2023.

Yang Li (Graduate Student Member, IEEE) received the B.Sc. degree in manufacturing engineering from Southwest Jiaotong University, Chengdu, China, in 2011, and the M.Sc. degree in material science and engineering from Washington State University, Pullman, WA, USA, in 2014. She is currently working toward the Ph.D. degree in power electronics packaging with Spellman High Power Electronics Lab, ECE Department, Stony Brook University, Stony Brook, NY, USA.

Before returning to academia, she had been a Reliability Engineer and Supervisor of Package Development and Simulation team dedicated on packaging optimization in the phase of new package design as well as debugging of packaging failures during the stages of mass production and reliability tests in Monolithic Power Systems, Chengdu, China. Her research interests include 48–1 V point of load converter design and high-voltage power electronics module for transportation and power grid applications.

Stig Munk-Nielsen (Member, IEEE) received the Ph.D. degree in power electronics from Aalborg University, Aalborg, Denmark, in 1997.

He is currently a Professor with AAU Energy, Aalborg University. His research interests include Si, SiC, and GaN components operating in soft and hard switching circuits, design challenges for low- and medium-voltage power modules, and converters with intended application in the industry.

Fang Luo (Senior Member, IEEE) received the Ph.D. degree in power electronics from Huazhong University of Science and Technology, Wuhan, China, in 2010, jointly supervised at Virginia Tech, Blacksburg, USA. He is currently an Empire Innovation Associate Professor and the Director of Spellman High Voltage Power Electronics Laboratory, Stony Brook University, Stony Brook, NY, USA. From 2014 to 2017, he was a Research Assistant Professor with The Ohio State University, Columbus, OH, USA. From 2017 to 2020, he was an Assistant Professor with the Electrical Engineering Department, University of Arkansas, Fayetteville, AR, USA. His research interests include high-power-density converter design, high-density electromagnetic interference filter design and integration, and power module packaging/integration for wide bandgap devices.

Dr. Luo was a recipient of the NSF CAREER Award. He is an Associate Editor for IEEE TRANSACTIONS ON POWER ELECTRONICS AND INTERNATIONAL TRANSACTIONS.